2021

A HAND-HELD STRUCTURE FROM MOTION PHOTOGRAMMETRIC APPROACH TO RIPARIAN AND STREAM ASSEESSMENT AND MONITORING

Joseph M. Dehnert

Joseph Dehnert

A HAND-HELD STRUCTURE FROM MOTION PHOTOGRAMMETRIC APPROACH TO RIPARIAN AND STREAM ASSEESSMENT AND MONITORING

By

JOSEPH MICHAEL DEHNERT

B.S., Georgia Southern University, 2013

Thesis

Presented in partial fulfillment of the requirements for the degree of

Master of Science (Community and Environmental Planning) in Geography

The University of Montana

Missoula, MT

June 2021

Approved by:

Scott Whittenburg, Dean

Graduate School

Dr. David Shively, Chair

Department of Geography

Dr. Lisa Eby

Department of Ecosystem and Conservation Sciences

Dr. Douglas Brinkerhoff

Department of Computer Science

Kevin McManigal

Department of Forest Management

PAGE INTENTIONALLY LEFT BLANK FOR COPYRIGHT INFORMATION

Dehnert, Joseph, M.S., Spring 2021 Major *Geography*

A hand-held structure from motion photogrammetric approach to riparian and stream assessment and monitoring

Chairperson: Dr. David Shively

Two of the biggest weaknesses in stream restoration and monitoring are: 1) subjective estimation and subsequent comparison of changes in channel form, vegetative cover, and in-stream habitat; and 2) the high costs in terms of financing, human resources, and time necessary to make these estimates. Remote sensing can be used to remedy these weaknesses and save organizations focused on restoration both money and time. However, implementing traditional remote sensing approaches via autonomous aerial systems or light detection and ranging systems is either prohibitively expensive or impossible along small streams with dense vegetation. Hand-held Structure from Motion Multi-view Stereo (SfM-MVS) photogrammetric technology can solve these problems by offering a resource efficient approach for producing 3D Models for a variety of environments. SfM-MVS photogrammetric technology is the result of cutting-edge advances in computer vision algorithms and discipline-specific research in the geosciences. This study found that images taken by GoPro, iPhone, and Digital Single-Lens Reflex cameras were all capable of producing 3D representations of heavily vegetated stream corridors with minimal image post-processing using workflows within Agisoft Metashape™. Analysis within Agisoft Metashape™ produced expected measurements from 3D textured mesh models, digital elevation models, and orthomosaics that were comparable to the physical measurements taken at the time of each survey using an arbitrary latitude, longitude, and elevation classification scheme. The methods described in this study could be applied in future stream restoration and monitoring efforts as a means to complement in person collection and measurement while limiting effort andmoney spent.

ACKNOWLEDGEMENTS

Thanks go out to everyone who helped with the development and implementation of this project. David Shively for his constant willingness to provide feedback and edits at each stage of the thesis. My partner Julie Heaton for being a sounding board and research assistant during an unusual COVID-19 season. Kevin McManigal for helping to streamline my research questions and make a more feasible study. Lisa Eby for asking the right questions during my defense; leading to a more complete project. To Doug Brinkerhoff for recommending I include the GoPro camera in this study and helping me understand some of the fundamental concepts of Structure from Motion. Finally, to my family and friends for supporting me and encouraging me to undertake this daunting process.

Table of Contents

List of Figures

List of Tables

1. Introduction

Because riparian zones serve as the interface between terrestrial and flowing freshwater ecosystems, it is important to identify and quantify their structural and functional roles in natural systems and monitor the restoration efforts being implemented (Nilsson et al. 1997; Capon et al. 2013). Over 37,000 stream restoration projects were reported in the United States between 1980 and 2005, but only 38% of those projects reported some sort of monitoring; 70% of those being monitored reported that the restoration actions were not accomplishing their intended purposes. (Bernhardt et al. 2005; Gloss and Bernhardt 2007; Conniff 2014). A rigorous understanding of the connection between riparian, geomorphic, and hydraulic processes provide a sound ecological foundation when identifying stream management objectives and evaluating current, and future, land-use practices (Gregory et al. 1991; Naiman et al. 1993). However, implementing studies that provide that framework typically demands a high cost in terms of financing, human resources, and time (Wen et al. 2017). This is especially true when carrying out and monitoring stream restoration efforts.

Two of the biggest weaknesses in current stream restoration and monitoring are: 1) subjective estimation and subsequent comparison of changes in channel form, vegetative cover, and in-stream habitat; and 2) the high costs in terms of financing, human resources, and time necessary to make these estimates (Wen et al. 2017). Hand-held Structure from Motion Multi-view Stereo (SfM-MVS) photogrammetric technology-based methods might solve these problems by offering a resource efficient approach for producing 3D visualizations for a variety of environments (Snavelly et al. 2008, Carrivick et al. 2016). SfM-MVS photogrammetric technology is the result of cutting-edge advances in computer vision algorithms and discipline-specific research in the geosciences (Triggs et al. 2000). By expanding the application of hand-

held photogrammetric technology to stream assessment and restoration monitoring projects, it should be possible to both increase and improve data collection in terms of accuracy and efficiency. To test this assertion, this study will test the feasibility of hand-held SfM-MVS photogrammetric data capture (herein 'Capture') as a flexible, efficient, and reliable means of providing locally referenced spatial data to stream assessment and monitoring efforts, and try to answer these questions:

1) What is the most suitable camera (cell phone, digital SLR, GoPro) for Capture in the field, considering minimum resolution, affordability, and error?
2) What is the most suitable image processing workflow, considering computing power and time constraints?
3) What measurements can Capture provide to stream restoration specialists and researchers?

This study utilized GoPro, iPhone, and Digital Single-Lens Reflex cameras to collect images along Rock Creek, Deer Creek, and Rattlesnake Creek. All three locations were chosen because of the size of the stream and the amount of vegetation present. The Rock Creek run was the pilot-study that served to test the feasibility of using the methodology in heavily vegetated environments. The Deer Creek run implemented the methodology tested at Rock Creek and determined the qualitative and quantitative measurements that Capture was able to produce. The Rattlesnake Creek run tested the same methodology but was carried out by a research assistant.

2. Background

The technologies and methods underlying the Capture methodology employed in this research stem from basic photogrammetry, computer visioning, fluvial geomorphology, and ecology. These are described here so that the study's methodological framework is firmly established before detailing the employment of Capture in the following Methodology section.

2.1 Terminology

Photogrammetry is the science and practice of making measurements from photographs. Structure from Motion (SfM) refers to algorithms used to produce three-dimensional point clouds from feature matched imagery for photogrammetric purposes. Multi-View Stereo describes the computer vision techniques that rely on SfM parameters to produce point clouds at a much finer scale that allows for discrete measurement of physical parameters in the scenes (Snavelly et al. 2008, Carrivick et al. 2016). The SfM process detects 2D features in each image and matches those features between pairs of images to create a coarse 3D mesh. Multi-View Stereo (MVS) techniques require those matched features to refine the coarse 3D mesh from SfM to a much denser 3D reconstruction in the form of 3D models like textured meshes, digital elevation models (DEMs), and orthomosaics. These products are typically georeferenced which places them in a specific coordinate system. However, in this study, the products were compared within the arbitrary coordinate system created within Agisoft Metashape™ using physical stream measurements between placed scale markers. Although there is no absolute definition for 'close-range remote sensing', the most widely agreed upon definition relates to images acquired from a distance of less than or equal to 300 meters on objects ranging from 0.5 meters to 200 meters in size (Luhmann et al. 2013).

Computer visioning software refers to the programs that contain tools, methods, and workflows for acquiring, processing, and analyzing digital images, and which allow extraction of high-resolution spatial data from real world imagery. This study employed the Agisoft Metashape™ computer visioning software, and the workflow is presented in the Methodology section that follows. Before delving into the technical SfM-MVS process, it is important to understand why photogrammetry and advancements in computer visioning now offer advantages for stream measurement and monitoring.

2.2 Riparian and Stream Restoration

The entire concept of ecological restoration is rooted in the idea that we can remedy past environmental damage by restoring the ability of the natural environments we have impacted to be shaped by the complex processes inherent within them. Stream restoration has been at the forefront of ecological restoration since the 1980s because streams are linked to issues ranging from water quality to endangered species. Beginning in the 1950s, geomorphologists began noting the connections between river channel morphology, flow processes, and sediment transport and began calling for the comprehensive measurements of river channel changes as a necessity for the development of proper management techniques (Horton 1945; Strahler 1952; Dietrich 1987; Lane et al. 1996; Lane 2000).

This created a demand for standardized measurement and classification protocols for fluvial landscapes, and resulted in various attempts at a 'one size fits all' approach to processes inherently rooted in a place-based context. The most predominant, though widely contested, stream classification scheme is the Rosgen (1994) method which sorts streams into categories of types and subtypes based on channel forms, slope angle, and substrate size. The Stream Visual Assessment Protocol (SVAP) co-created by the United States Department of Agriculture

(USDA) and the Natural Resources Conservation Service (NRCS) incorporates the Rosgen method into the first level of its ecological assessment protocols, and ocular measurements include water surface and flow observations that allow channel units identification (e.g., pool, riffle, run), channel depth, channel width, and substrates among others (NRCS 2010).

Although the SVAP protocol is practical and provides invaluable data, it requires a significant time commitment from both trainers and trainees, and doesn't provide a comprehensive visual picture of the stream at the time of survey (HLA 2020). Additionally, determining the variance and error corresponding to ocular estimations by different research technicians proves difficult. To resolve this difficulty physical stream surveys have been continuously perfected since the 1950s resulting in more standardized ways to measure and quantify changes in fluvial landscapes describing channel morphology, habitat, flow processes, and sediment transport. This rings true for assessments like the HLA which are updated every 5 years to reflect changes in standards for estimation (HLA 2020)

2.3 Stream Monitoring

Establishing an objective 'baseline' at the beginning of a restoration project is extremely important for long-term monitoring efforts (greater than 25 years) allow for the determination of rate and trajectory of change, effectiveness, and success, but acquiring robust stream measurements is prohibitively expensive for large-scale and/or long-term projects and in areas that are difficult to access (Angeler and Allen 2016). The most common alternative is comparison of the restoration project with a reference site that offers desired restoration targets and thus allows for assessment of recovery rates (Nauman et al. 2017). However, variability in natural landscapes, especially riparian environments, often hinders the identification of reference sites (Pickett and Parker 1994; White and Walker 1997). Therefore, the most recent approaches

to monitoring large expanses of fluvial landscapes, utilize remotely sensed images and photogrammetry to monitor changes to a landscape over time (Kennedy et al. 2014). These photogrammetric methods began emerging in the early 1980s and involved the interpretation of aerial imagery in conjunction with physical measurements, and were predominantly focused on floodplain studies using analog methods (such as described by Lewin and Manton 1975). However, documenting changes in stream structure and riparian vegetation with photogrammetry in heavily vegetated zones is either impossible or prohibitively expensive using current aerial and terrestrial remote sensing techniques. But with the advent of high resolution (hyperspatial) digital sensors, autonomous aerial vehicle (AAV) technology, and computer visioning software, remote sensing is being utilized to help standardize the way changes in stream structure and riparian vegetation is documented over time. A burgeoning solution to measuring and monitoring changes in stream structure and riparian vegetation in areas where traditional remote sensing methods cannot be implemented is the utilization of portable hand-held sensors in conjunction with SfM-MVS photogrammetry to create 3D 'snapshots' of a scene at the time of survey.

2.4 Digital Photogrammetry

Lane et al., (1994) and Lane (1998) began showing some of the applications of ground-based digital photogrammetry in the study of river channels, bank erosion, and gravel-bar surfaces in the 1990s, and photogrammetric applications have continued in tandem with image sensing technologies. Currently, ground based photogrammetric surveys can be conducted using cell phone, DSLR, and GoPro cameras and aerial photogrammetric surveys can implement AAVs. Digital photogrammetry can be georeferenced with total stations surveys or be used as a standalone tool. These surveys are cost efficient and can produce accuracy similar to total-station surveys (Westoby et al. 2012; Armistead 2013; Dietrich 2016).

There are two techniques for digital photogrammetry, close-range (< 300m from sensor to subject) and aerial (>300m from sensor to subject). Most close-range photogrammetry is done with the use of a DSLR or cell phone camera, and produces 3D models which can be developed to produce DEMs (American Society for Photogrammetry and Remote Sensing 2016). These 3D models are created by using at least 60% of the overlapping stereo pairs between images along with the known camera position parameters (James and Robinson, 2012). However, camera position, scene geometry, and keypoint identification are automatically determined when using a SfM-MVS approach to photogrammetry which makes it an invaluable solution to creating 3D models in areas where aerial sensors are impractical and terrestrial sensors like ground-based light detection and ranging (LiDAR) are prohibitively expensive.

2.5 Structure from Motion-Multi-View Stereo (SfM-MVS)

SfM has its roots in the computer visioning community, and was developed to track known points across suites of imagery from various positions to determine camera pose and scene geometry, and ultimately generate 3D models. The coplanarity and collinearity algorithms involved in this process have been developing since photogrammetry began rising to prominence in the 1980s, but the coplanarity algorithm was actually being applied in the 1950s and 1960s (Thompson 1965) when attempting to georeference and map surface features from aerial images. The image adjustment, which utilizes a collinearity algorithm to establish a geometric relationship between image and object, was developed in the early 1970s (Brown 1971; Kenefick et al. 1972; Granshaw 1980). Kenefick et al. (1972) actually developed a 'self-calibrating' image bundle adjustment algorithm that can model and estimate parameters even with distorted images from consumer grade cameras. The ability to assume that a different camera was used to

acquire every single image and calibrate each bundle individually was a breakthrough in the computer visioning world.

The question driving developments in SfM-MVS is, how can known points within varying images be extracted for accurate measurements while being simultaneously unaffected by changes in camera orientation, scale, illumination, or 3D position? (Carrivick et al. 2016). The first step in answering this question involves the pairing of common points or, keypoints, between different images. A wide variety of keypoint identifiers have been developed based on stereo matching statistics (Lucas & Kanade 1981) and identification of planar surfaces or features (Moravec 1983). Initially, all of the various methods utilized for keypoint identification were limited by the fact that they worked best when taken from a similar viewpoint, or at a similar scale (Snavely 2008). The challenge, once again, is rooted in the ability to track features between images taken from various perspectives. These challenges were first addressed by Baumberg (2000) and Matas et al. (2004) in a method known as wide base-line matching which prioritized feature points, or pixels, that change covariantly with scale and orientation. However, the method that rose to prominence became the scale-invariant feature transformation (SIFT) object-recognition system because it provides the most feature matches of various circumstances (Lowe 1999 2001 2004).

2.6 SfM-MVS Breakdown

SIFT is used as the first step in the Agisoft Photoscan 3D modeling process employed in this study, and it has four main steps. As noted in Carrivick et al. (2016) the first step is to determine the scales and locations in the image sets that can be used repeatedly from various perspectives.

Once stable parameters are determined a Gaussian function is applied to the images at various scales, producing a Gaussian-smoothed image, and each feature point within the image is compared to the eight neighboring feature points at each scale and to the neighbors in the selected scales above and below. Once the spatial extent of the images is identified, then the keypoint positions can be determined in space using their location, scale, and ratio in bundles of the various accepted spatial extrema. After establishing keypoints that work at preferred scales, a consistent orientation of each keypoint is assigned based on the scale closest to the dominant keypoint for each image. Alternate keypoints can be selected for each image but those points may have a different orientation for the preferred scale. Once the orientation and scale is defined then each main keypoint must be described in space, showing magnitudes of color gradient, to avoid being completely distorted when matched with itself from other images at different scales. Basically, a Gaussian weighting function window establishes the magnitude of gradients over a keypoint and then aggregates those gradients into descriptors which are invariant to scale but covariant to orientation and location (Carrivick et al. 2016). A keypoint descriptor is created by first computing the gradient magnitude and orientation at each image sample point in a region around the keypoint location, as shown on the left. These are weighted by a Gaussian window, indicated by the overlaid circle. These samples are then accumulated into orientation histograms summarizing the contents over 4x4 subregions, as shown on the right, with the length of each arrow corresponding to the sum of the gradient magnitudes near that direction within the region (Lowe 2004).

Once the keypoint positions have been identified, relationships between those keypoints from different images have to be determined in order to begin building a 3D point cloud. This is where study design is integral to 3D model quality because there is no guarantee that a keypoint will have a partner in another image unless dictated in the study design. The specific method chosen for this study uses clearly identifiable markers with a predetermined overlap in images to ensure quality keypoint correspondence; it will be discussed in detail in the Methodology section below. The most efficient way to match keypoints between various imagery is using Euclidean distance of the nearest neighbor with that of the second nearest, specifying a specific value or 'distance ratio' (Lowe 2004; Snavely et al. 2008). This ratio has been shown to get rid of over 90% of the false matches while only including 5% of the correct matches in the elimination process. This method has also been found to perform better than a global distance threshold, and even the false matches are unlikely to be weighted as correct matches given the fact that Euclidean distance has options that are more or less correct based on distance (Lowe 2004).

In an effort to ensure collinearity is preserved as images become transformed a relationship must be specified between the correctly identified keypoints in each image. To establish this line where all points remain unchanged regardless of transformation it is important to get rid of the noise surrounding each keypoint using random sampling methods to place keypoints into geometrically consistent matches. There are various methods utilized in this step of image processing, but they all work by taking random samples of keypoints and establishing estimations of inliers or outliers based on the least square fit of the smallest subsets. These estimations are then applied to larger subsets until a certain percentage of the noise surrounding each keypoint is selected to be kept or not. Once the outliers have been eliminated and collinearity has been established between keypoints across images, the SfM step can begin.

Although the entire process described above is often referred to as SfM, the reality is that SfM describes the specific step in the image processing workflow where 3D geometry (structure) and camera poses (motion) are determined (Ullman 1979). SfM aims to simultaneously estimate the 3D scene structure, camera poses and orientations (external parameters), and focal length, principal point, and radial distortion (internal parameters). Scene reconstruction usually begins by pairing two images based on a feature present in both images which can easily be identified and has a strong collinear baseline from vastly different perspectives. Snavely et al. (2008) shows that having an easily identifiable feature between two images where focal length estimates are available makes obtaining the remaining camera parameters much easier with bundle adjustments.

Bundle adjustments are the 'bundles' of light rays that connect camera centers to 3D points with a minimal re-projection error (Szeliski 2011). Once re-projection error between each image has been minimized, then multiple cameras can be added into the optimization process. In most cases a new camera, or perspective, is chosen if it contains a keypoint with at least 75% match to an already selected camera. The external parameters for each additional camera can then be estimated using a direct linear transformation technique (Abel-Aziz and Karara 1971). This technique takes the existing 3D coordinates of the matched pair and produces a set of 2D coordinates for each new camera. The 2D coordinates are then projected into 3D object space using bundle adjustments for determining how keypoints in the newly projected image relate to previously established cameras. This is a useful transformation because it only allows the newly projected camera parameters and the keypoints it observes to change in 3D space by specifying a maximum angle threshold beyond which the location of the point will be rejected. The camera

will have to go back through the re-projection process before the keypoints contained in its perspectives are incorporated as a baseline perspective.

If bundle adjustment tracks between images have a high re-projection error, they are removed in the SfM process. The best way to determine if all of the selected camera perspectives have a low re-projection error is to run a global re-adjustment before moving onto the scale and georeferencing phase. This global bundle adjustment scans the reconstructed 3D points offered by each camera to ensure that there are no remaining perspectives that can be reliably added to the model, and at this stage shouldn't require extra computing power because the individual bundle adjustments have already occurred. Once completed, the SfM process produces a sparse point cloud and the camera poses. However, discrete distances between images or reconstructed points are unable to be recovered from images alone, and thus georeferencing and scaling of the point cloud is required (Szeliski 2011).

To georeference a point cloud, most programs require a minimum of three ground control points (GCPs) or known camera positions derived from real-time kinematic differential GPS (rtkGPS) measurements. Having established rtkGPS targets in each image is the most commonly used method for georeferencing images because it allows users to specify the target coordinates in post-processing of the images (M.R. James and Robson 2012). Once these known coordinates are established the bundle adjustment, the SfM, step can be utilized again to further optimize 3D geometry. To optimize 3D geometry and the resulting models, additional MVS algorithms are utilized especially in projects with large datasets because the clustering and patch adjustments break the image sets into 'chunks' based on global affinity values between images. These algorithms basically construct an individual depth map, or 3D scene for each cluster of imagery and then merge the separate maps to create a dense, clean, 3D geometry (Furukawa et al. 2010).

There are a host of different MVS algorithms that typically fall into four different categories; 1) voxel-based (S.M. Seitz and Dyer 1999); 2) mesh change (Furukawa and Ponce 2009); 3) geometry merging (Li et al. 2010); and 4) patch-based (M. Lhuillier and Quan 2005). The one utilized in this study will be the patch-based MVS algorithms (PMVS) because it is used in Agisoft Metashape™ and matches features using small patches (surfels), expands the patches of matched images, and then filters out incorrect matches. This is the most critical step in the SfM process because it relies on defined texture information for each surfel to produce a 3D model than can be transformed into a comparable DEM. If there are inconsistencies between surfels then the PMVS algorithms filter out that set of points creating a gap in the 3D model. The surfel matching, expansion, and filtering steps are repeated several times before the final, dense, point cloud is created. This PMVS method allows for dense reconstructions of objects while requiring minimal computing power and time. However, the key constraint to the entire SfM-MVS process is pixel-level feature detection within source imagery, especially in areas with ever-changing objects or scenes (Gruen 2012).

2.7 Photographic Considerations

Both Lane (2000) and Gruen (2012) argue that pixel matching is the critical consideration when attempting digital photogrammetry and automated modelling. The quality of the pixels is dependent on factors like image quality, lighting conditions, and object texturing. As described above, pixel matching is key to the entire SfM-MVS process and quality matching can increase point densities by over two orders of magnitude (Smith et al. 2016). Micheletti et al. (2015) has shown that a variety of camera systems can produce quality pixels and high pixel matching. Micheletti et al. (2015) was able to create digital terrain models (DTMs) with decimeter accuracy

using a smart phone camera at close range, but also showed significant accuracy improvement using a DSLR camera system.

Micheletti et al. (2015), Fondstad et al. (2013), and Dietrich (2016) found that close-range coverage, 5-15 meter, produces optimal results when capturing images for SfM-MVS photogrammetry. However, there is an inverse relationship between sensor distance from subject and the minimum number of images required to cover the spatial extent and topographic complexity in a scene; the closer the sensor distance to subject the more images necessary which requires more computing power than aerial surveys (Smith et al. 2016).

2.8 Historical Uses

The predominant application of SfM-MVS photogrammetric technology is in land-form terrain modeling via AAVs (Fonstad et al. 2013). Over the past two decades, close-range digital photogrammetry has become a powerful tool for 3D terrain modelling, and has enabled the monitoring of river beds, river banks, glaciers, and much more at relatively high spatial resolution through the extraction of DEMs from overlapping stereo imagery. The traditional methodology has been to equip an AAV with a camera that has stable focal length, principal point, and lens distortion parameters (e.g. a metric camera) to acquire imagery that can be used for photogrammetric measurement (Bird et al. 2010). Recently, advances in high-resolution satellite image-matching techniques and machine learning algorithms have been used to create cost-effective, moderately scaled approaches to terrain modelling without the need to invest valuable resources in AAV specialization (Stumpf et al. 2015). However, these advanced remote sensing approaches cannot provide hyperspatial data in dynamic riverine environments and thus, field-deployable, close-range photogrammetric methods must be used to measure the subtle changes occurring within the riparian zone.

2.9 Advantages and Disadvantages

Seemingly, the biggest attraction for using a close range hand-held SfM-MVS photogrammetric approach to riparian and stream assessment and monitoring is that it should be very cheap in terms of personnel and time constraints, compared to other survey methods. The only requirements are a camera and a computer. There are free software options available online, and countless professional options that are moderately priced. Furthermore, SfM-MVS produces fully 3D data which has typically only been possible with a terrestrial LiDAR scanner (TLS), and these data can be very easily transformed into orthophotographs and DEMs (Bemis et al. 2014). Additionally, the SfM-MVS workflow remains relatively unchanged regardless of spatial or temporal scales. This fact bodes well for this study because it can draw upon the work done in various environments from different scales and incorporate it into designing a study for a close range approach in heavily vegetated riparian environments. Lastly, as seen in Carrivick et al. (2016) SfM-MVS workflows can produce similar accuracy to almost any other topographic surveying method. The comparisons to Terrestrial Lidar Survey (TLS), Aerial Lidar Survey (ALS), and differential GPS (DGPS) show that photogrammetry and SfM-MVS values are completely dependent scale of investigation (e.g. landscape vs. site scale) (Brasington et al.2000; Young 2013; Gallay 2013; Bangen et al. 2014; Carrivick 2016).

The biggest disadvantage to the SfM-MVS approach to digital photogrammetry is the fact that 3D accuracy and 3D point density often depends on factors that surveyors can't control like ambient lighting, texture, and color of the object or scene of interest (Fondstad et al. 2013; G.A. Gienko and Terry 2014). This issue means that repeating a particular SfM-MVS workflow can be challenging especially when the surveyor has to make situation specific adjustments due to the conditions at the time of sampling. Additionally, objects or scenes that move between

each image capture (vegetation blowing in the wind) can't be surveyed using a rigid workflow. While the majority of the SfM-MVS data acquisition and processing can be done by a relatively unspecialized user, certain complementary data like rtkGPS and physical stream measurements help to create more robust 3D data, and require more specialized skills. Another disadvantage is the fact that points cannot be attributed at the time of survey like total station surveys. Lastly, the visualization of large datasets can be very difficult especially if the steps prior to PMVS cannot produce quality image pairs. In general, the future of the SfM-MVS process in digital photogrammetry largely depends on applying advances in technology to real-world field applications to test the 'best-fit' methods for surveying different environments.

3. Methodology

This research included both field and lab components for data collection and processing. Unfortunately, there is a large gap in the current literature when it comes to study designs centered on close range hand-held photogrammetric approaches to riparian and stream assessment and monitoring. Particular care was taken to develop and employ an easily reproducible study design, including the field and lab components as this relates directly to the research questions. All lab work was done using University of Montana computers and software licenses.

3.1 Transect and Image Acquisition

The field component of this research was altered by the COVID-19 research protocols released by the University of Montana on 1 June 2020. The following methodology was employed at three different locations along Deer Creek, located in Mineral County, Montana. Prior to the commencement of fieldwork at Deer Creek, the methodology was pilot-tested on an

irrigation canal along Rock Creek, located in Missoula County, Montana (see Figure 1 below). To allow scaling for each image, and provide boundaries for physical measurement, at least coded three targets were placed on each side of the channel, and were equally spaced throughout each transect (along the side of the channel) (Micheletti et al. 2014). A step-by-step approach to image acquisition and physical stream survey is outlined in Table 1 below.

Table 1. Basic Image Acquisitions and Physical Measurement Methodology

1. Select a heavily vegetated section of stream approximately 20 meters long.
2. Place laminated markers along streambank with coded targets all facing the same direction.
3. Facing the coded targets, hold camera in landscape orientation (sideways), at chest height.
4. Walk along the center of the stream taking at least 1 photo every step. The camera can pan left and right as needed to capture targets or objects of note on either side of the channel, but should always include at least one target in every photo.
5. Obtain section length, wetted width, and distance between markers using meter stick and measuring tape.
6. Catalog average size of rocks in stream and along the bank.
7. Catalog dominant vegetation type (trees, grasses, shrubs, etc.)
8. Catalog dominant species of vegetation if known.

The placement scheme for marker locations is limited only by the requirement to have at least 3 markers present in each image. Where that is impossible, having at least one marker is necessary. There are no other restrictive parameters for marker placement such as known locations or predetermined distances. The rationale behind this lies in the photogrammetric process of keypoint identification. The markers serve two purposes: 1. Providing reference points for real world scale and 2. Providing reference locations for keypoint identification.

3.2 Rock Creek Pilot Test

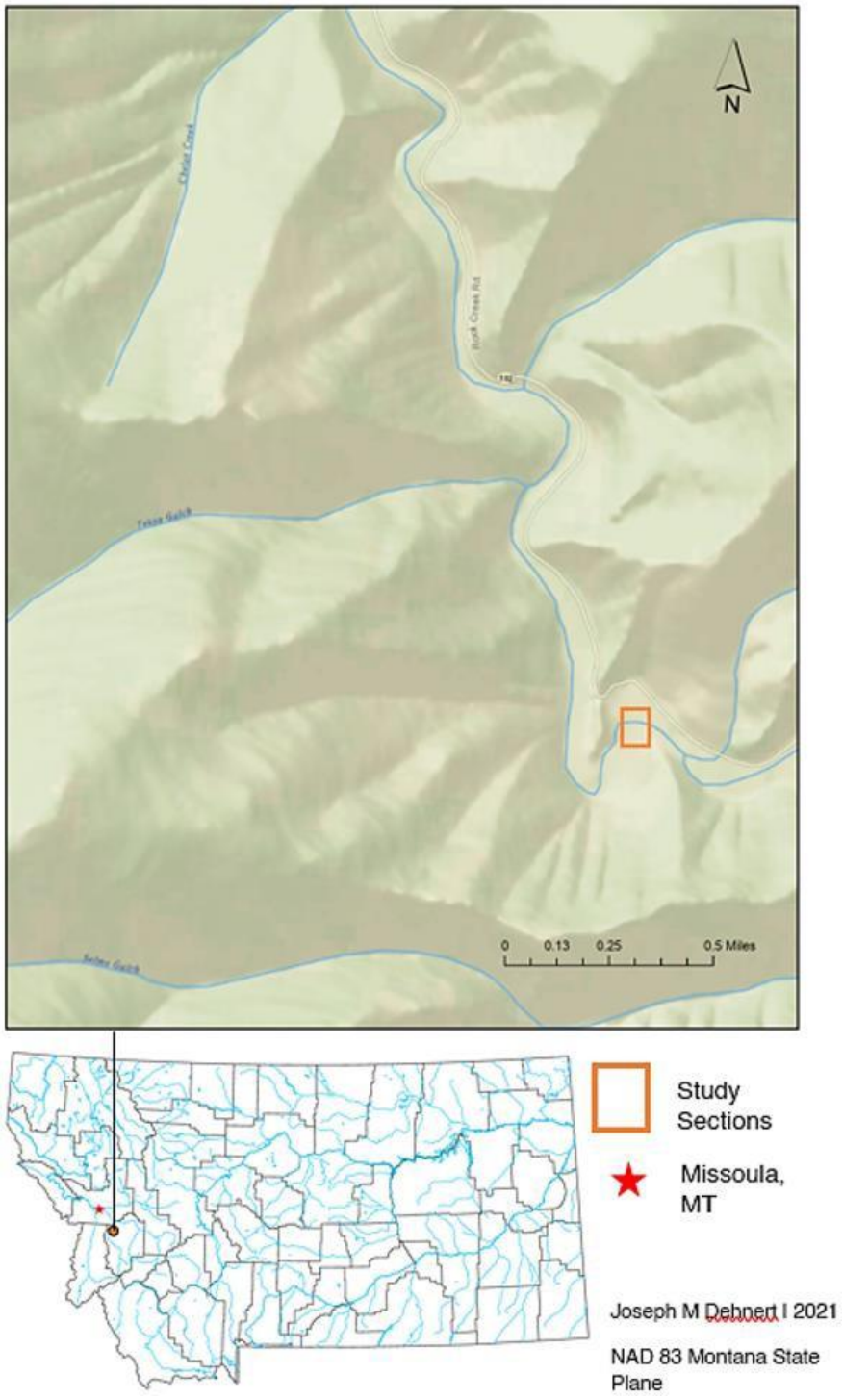

Figure 1. Rock Creek Pilot Test Locator Map

The basic image acquisition and physical measurement methodology described above was tested using a Sony a6500, iPhone 6 SE, and a GoPro Hero 4 along irrigation canals that feed into Rock Creek near Clinton, Montana and proved successful.

Figure 2. Rock Creek Pilot Test Images. Note: Pilot test photos represent how images are taken with rotating the camera laterally.

The focal length of the Sony a6500 created issue when photographing the riparian zone; the stream and identifiable targets were largely absent from the images which prevented quality matching within Agisoft Metashape™. Therefore, because one of the cameras was unable to adhere to a rigid transect and image acquisition structure a more 'free-form' structure was employed. This idea of 'free-form' image acquisition is rooted in the literature and simply indicates complete coverage of the study area by taking as many photos as possible from every angle (Micheletti et al. 2015). This approach complemented this study's focus on the unspecialized user as it dictates a simple 'walkthrough' of the site of interest taking more photos than one might believe to be necessary.

3.3 Deer Creek Run

A comprehensive physical stream survey occurred during the Deer Creek survey at the same time Capture data were being collected to provide physical measurements for comparison with Capture measurements derived from 3D models. The physical survey parameters adhered to the NRCS method for determining the following in-channel and riparian characteristics at each transect. See Table 2 below. The Deer Creek sampling took place during typical summer flows on July 7th and August 8th. Having two samples occur in quick succession helped to resolve the gaps in data collection and synchronize the software workflow.

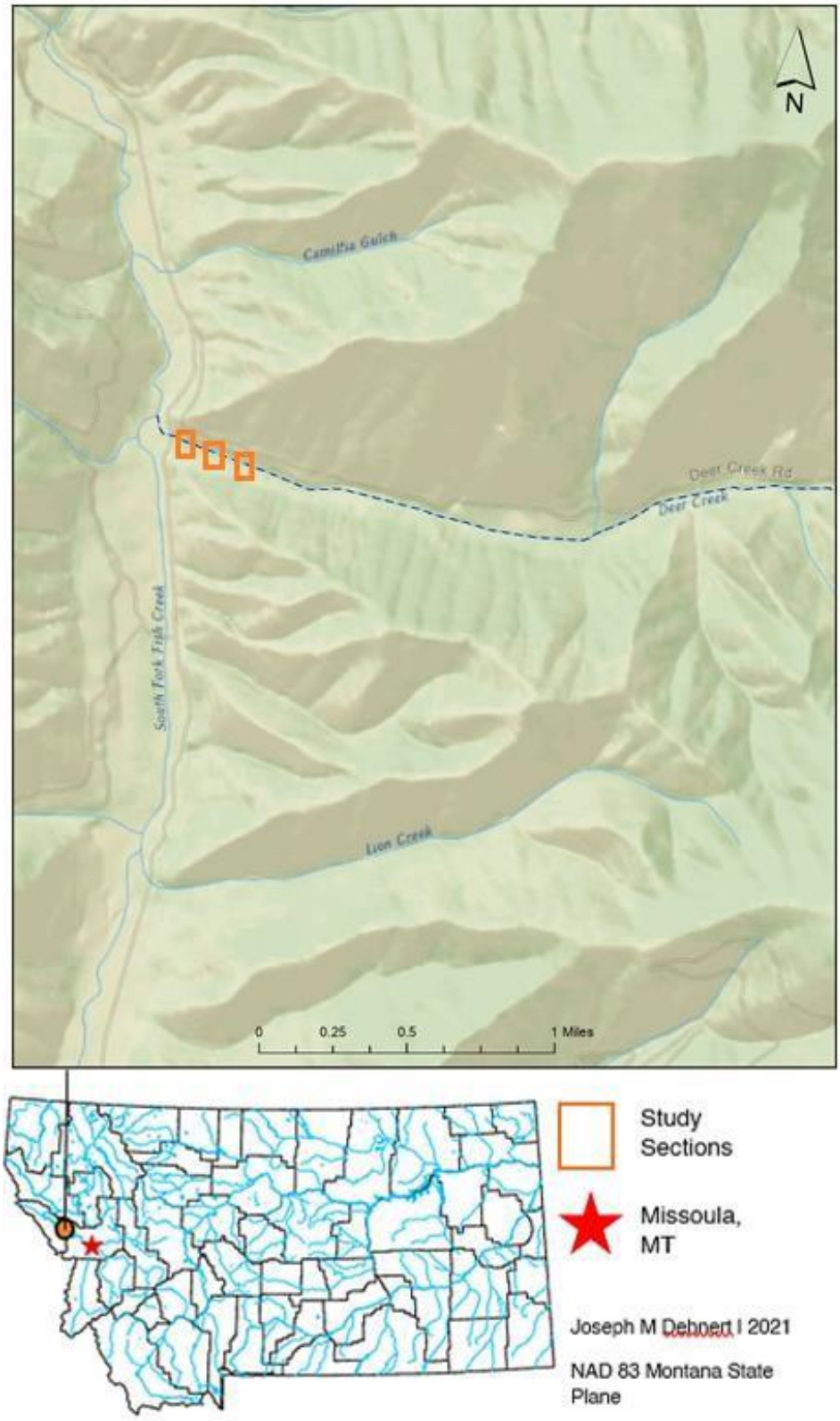

Figure 3. Deer Creek Run Locator Map

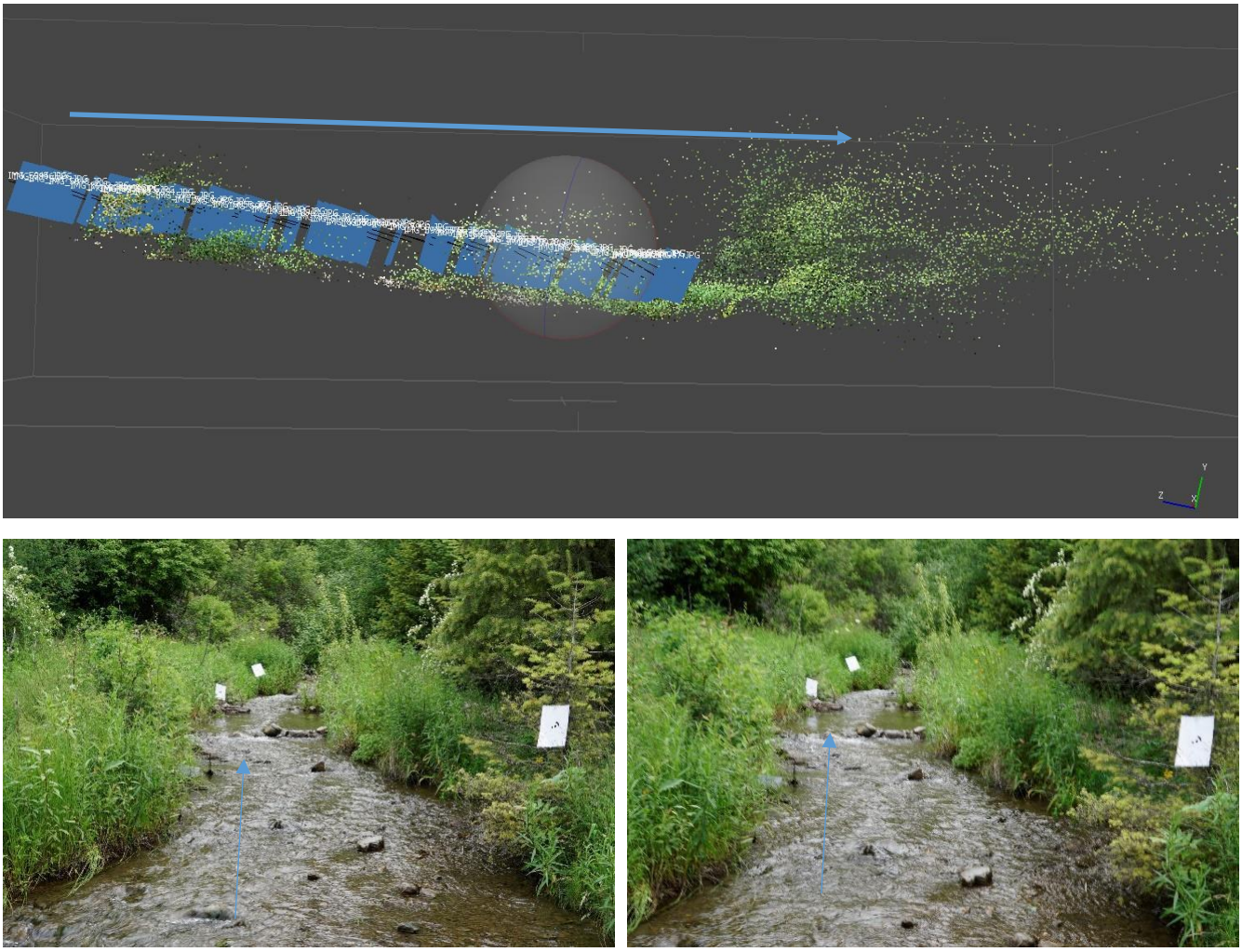

Figure 4. Deer Creek Run Images. Note: the top image (a) shows the point cloud created in Metashape™ with the blue arrow showing the direction walked in the stream and the images taken with the DSLR camera displayed as the blue rectangles within the point cloud. The bottom left and right images (b and c respectively) show the same blue arrow signaling walking direction upstream as the images were taken.

Table 2. Physical Stream Measurements for Deer Creek and Rattlesnake Creek Runs

1. Classify/catalog habitat type (pool, riffle, glide);
2. Classify riparian vegetation (list species and estimate abundance of each);
3. Measure wetted channel width;
4. Determine average water depth in section (includes >=5 measurements of depth in each section);
5. Average streambank substrate size (includes >=5 measurements in each section);
6. Estimate vegetative percent cover of each streambank (extending 5m from water's edge);
7. Measure bank slope;
8. Measure channel incision;
9. Describe bank stability classification (Stable w/ vegetative cover/non-erosive; Unstable w/ eroding and/or bare soil; Hardened w/ concrete, riprap or bedrock).

3.4 Rattlesnake Creek Run

The purpose of the Rattlesnake Creek study was to determine the ease and accuracy with which the proposed methodology and workflow could be implemented by an unspecialized user. A research assistant was given the following instructions and used the same iPhone camera used in the Deer Creek Survey. The Rattlesnake Creek Sample took place during typical low winter flow conditions on 24 January, 2021.

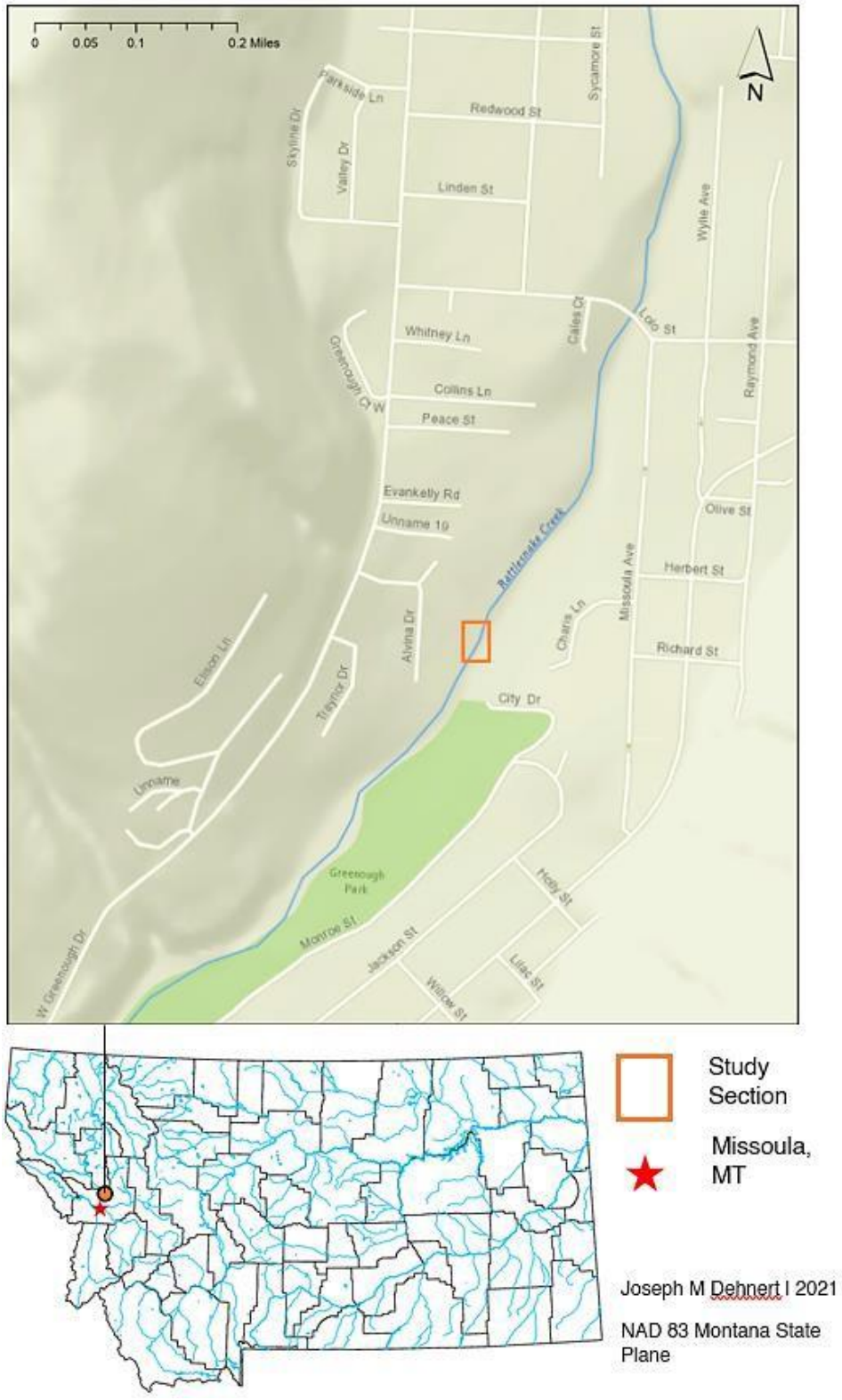

Figure 5. Rattlesnake Creek Run Locator Map

Figure 6. Rattlesnake Creek Run Images

3.5 Image Acquisition

The vast majority of SfM-MVS processes produce internal and external camera calibration models as mentioned above, but field-based calibrations can help to make the models produced in the software more accurate. In an effort to minimize inaccuracies in environments where extreme variability between image captures is likely to occur the following guidelines from Peterson et al. (2015) were adopted:

Table 3. Camera Parameter Guidelines

Lens: a fixed focal length lens.
Camera Settings: aperture was set to constant intermediate f-stop between f/8 and f/16 depending on ambient light and shadows, and ISO were set as low as possible with a shutter speed of at 1/400 of a second; Camera Focus: focus was set at a constant, but where focus was altered an additional image was captured of a different scene to mark a spot in the photo sequence where the focus was changed (this resulted in a different camera being selected in Agisoft Metashape™ workflow);
Camera Resolution: the highest possible resolution was used for sharpness and depth-of-field to be maintained; (low iso, high apperature)
File Format: for the DSLR camera a RAW (+JPEG) format was used in an effort to create flexibility in bright or dark areas of images and to prevent data loss due to file compression;
For cell phone camera, the highest quality compression level was used and no rolling shutter will be used for any image acquisition.
GPS: for the cell phone camera, the internal GPS was used to guide the initial 3D model creation, and a hand-held GPS device was used for the DSLR camera unless (in the case of cell phone camera and hand-held GPS devices, accuracy was accounted for in Agisoft Metashape™ settings).

Images were captured with 24 MP Sony a6500 (herein Sensor A) equipped with a fixed focal length (xx mm) Nikon lens. Sensor A has a crop factor of 1.5 which gave the 35mm fixed lens an equivalent 50mm field of view. Sensor A also has the capability to save in RAW file formats which aided in post-processing (Micheletti et al. 2015). Shutter speed on Sensor A ranges from 1/4000s of a second to 30 seconds. For this study a standardized shutter speed, aperture, and flash was used for each image in an attempt to limit the variability present in close range remote sensing. ISO was locked at 100, and shutter speed was locked at 1/40th of a second with aperture being locked at *f*-8.

The average distance between images taken at all 3 sites varied between 1-3 meters depending on terrain to ensure stereo imagery pairs with at least 60% overlap (with the long-axis of the image perpendicular to image path) (Bird et al. 2010). In an effort to keep this research aligned with its primary goal of being stakeholder focused, I utilized the 'black-box' algorithms provided in Agisoft Metashape™ that estimate the parameters mentioned above and only manipulated those parameters if necessary. Camera height was difficult to standardize, but remained at roughly 'chest height', approximately equal to a standing eye height (2 m off the ground). The relative height of the camera at the time of survey should bear very little weight because the oblique angle of the images will not change much between an image taken 1.5 m off the ground and 2 m off the ground.

Distance from objects like logs or other instream habitat features varied depending on distance from the last photo and viable walkways around the features. Extra care was taken when capturing images of logs, boulders, cut banks, and vegetation to maximize the chances of stereo pair matching.

Because the object distance (from sensor to features) could be approaching zero from certain perspectives, resulting in an out-of-focus image, the far-point and near-point for focus was set at infinity on Sensor A. This fixed some of the depth-of-field issues in images with no real object of interest.

3.6 Lab Component

The lab component used Adope Photoshop for image processing and Agisoft Metashape™ for 3D visualization creation. The final workflow was chosen based on the quality of data required/produced and ease of operation at each of the following steps:

Table 4. Image Pre-processing Workflow

The following image pre-processing workflow was used and is adopted from professional SfM-MVS workshop by Tommy Noble (2018):
Download all photos and organize into appropriate folders based on survey design.
Balance color and exposure and remove vignetting and chromatic aberration via AP.
Back up all original and balanced images.
Export balanced images as JPEG, TIF, or DNG.

For a more descriptive application of the following Agisoft Metashape™ workflow please see Figure 7 which lists the specific workflow adopted by the United States Geological Survey in 2017.

The following Agisoft Metashape™ error minimization workflow was used once image pre-processing was completed and is adapted from a professional SfM-MVS workshop provided by Tommy Noble (2018):

Table 5. Agisoft Metashape™ Error Minimization Workflow

Add images to Agisoft Metashape™ and check EXIF info;
Sort images by Capture group to help project organization;
Create camera calibration groups for proper calibration;
Align images using keypoint triangulations to create a sparse point cloud;
Optimize point cloud by performing 1st bundle adjustment;
Add a scale using the coded targets from each image;
Optimize point cloud by performing 2nd bundle adjustment;
Perform projection accuracy gradual selection to remove points with undesirable residual error (RE);
Perform reconstruction uncertainty to remove points with undesirable RE;
Perform reprojection error to remove points with undesirable RE;
Optimize point cloud by performing 3rd bundle adjustment removing points with >0.3RE;
Adjust results from final optimization to fall within 0.13 to 0.17 RMSE;

Agisoft PhotoScan Workflow

Steps	Menu	Function	Action
Photo Setup, Alignment, Adjustment			
1	Main Menu - Workflow	Add Photos	Navigate to directory with photos. Select and add all necessary photos for project
2	Reference Panel - Settings	Set Coordinate/Projection	Select the Coordinate System (Local, Geographic, Projected) and Select Projection (i.e. WGS84)
3	Main Menu - Tools	Camera Calibration	Check to make sure that all the photos with the same focal distance/parameters are grouped together
4	Main Menu - Workflow	Align Photos	Settings: high, generic or referenced, 60,000, 0
5	Reference Panel - Optimize	Initial Bundle Adjustment	☑ *Check on: f, cx, cy, k1, k2, k3, p1, p2*
Error Reduction & Bundle Adjustment			
6	Main Menu - Edit Gradual Selection	Reconstruction Uncertainty (Geometry)	Set Level: 10 (if more than 50% of pts are selected, increase the level to a higher value (limit 50))
			Delete the points, Optimize
			☑ *Check on: f, cx, cy, k1, k2, k3, p1, p2*
			Repeat and least 2 times and continue to lower the level closer to 10 without having to delete points
			Monitor: Projections goal not less than 100, Error (pix) goal = .3, SEUW = 1.0
7	Main Menu - Edit Gradual Selection	Projection Accuracy (Pixel Matching Errors)	Set Level: 2 - 3 (if more than 50% of pts are selected, increase the level to a higer value (i.e. 3))
			Delete the points, Optimize
			☑ *Check on: f, cx, cy, k1, k2, k3, p1, p2*
			Repeat and least 2 times and continue to lower the level closer to 2 without having to delete points
		Tighten Tie Point Accuracy Value	Change the settings of the tie point accuracy (pix) from 1 to .1
			Optimize
			☑ *Check on (all): f, cx, cy, k1, k2, k3, k4, b1, b2, p1, p, p3, p4*
			Monitor: Projections goal not less than 100, Error (pix) goal = .3, SEUW = 1.0
8	Main Menu - Photo Edit Markers	Add Control Points (Markers)	Import in the ground control points (if available), manually select or use autodetection on individual images
		Add Scale Bars	Select the Coordinate System (Local, Geographic, Projected) and Select Projection (i.e. WGS84)
9	Main Menu - Edit Gradual Selection	Reprojection Error (Pixel Residual Errors)	Set Level: .3 (if more than 10% of pts are selected, increase the level to a higher value)
			Delete the points, Optimize
			☑ *Check on (all): f, cx, cy, k1, k2, k3, k4, b1, b2, p1, p, p3, p4*
			Repeat until reaching the .3 level without having to delete points
			Monitor: Projections goal not less than 100, Error (pix) goal = .3, SEUW = 1.0
Build Dense Point Cloud, Mesh, Texture, DEM, Orthomosaic			
10	Main Menu - Workflow	Build Dense Cloud	Quality: High, Med, Low Depth Filtering: Agressive
		Build Mesh	Height Field, Dense cloud, High Interpolation: Enabled
		Build Texture (optional)	Orthophoto, Mosaic
		Build DEM	Set Coordinate System/Projection, Dense Cloud, Enabled
		Build Orthomosaic	Geographic, Set Coordinate System/Projection, Mesh, Mosaic

USGS National UAS Project Office – March 2017

Figure 7. Agisoft Metashape™ Workflow developed by Tommy Noble for the USGS (Source: Noble 2018).

3.7 Lab Component Alterations

Because the images taken during the time of survey were not georeferenced a new workflow had to be created to compare changes between spatial products produced without geospatial information. To do this, a standardized local coordinate system was first created. This local coordinate system was creating by first exporting all of the known camera positions following the final bundle adjustment. By exporting the local coordinate system created by the optimized cameras, the x,y,z locations could then be imported back into the Metashape™ workspace, giving the model a means of comparison. However, to compare one model to another, they both had to be in the same workspace. Within Metashape™, workspaces are organized as follows:

Table 6. Agisoft Metashape™ workspace organizational scheme.

Chunk (term used to define a group of cameras)
Cameras (term given to each individual image. i.e., 20 images = 20 cameras)
Keypoints (this defines the total number of points used in dense cloud creation)
Products (the rest of the workspace is organized by products created. i.e., DEM, 3DMESH, ORTHOMOSAIC, etc.)

To get multiple models within the same workspace, new Chunks have to be added. This is done by selecting the workspace of choice and manually adding new Chunks and Cameras. Once the workflow outlined in Figure 7 above was completed in the newly created Chunk, the DEMs could be compared using the 'Transform DEM' tool present in Metashape™. This tool created an elevation difference map with appurtenant data. The addition of this tool to the lab component in this study enabled non-georeferenced change comparison.

4. Results

The results of this study detail the products and findings of using Capture along heavily vegetated small streams as a complimentary method to traditional stream surveys. For each section of stream, images were analyzed and dense clouds, 3D meshes, DEMs, and Orthomosaics were created within Agisoft Metashape™. The root mean square error (RMSE) was used as the primary indicator of model quality. Prior to the gradual selection steps which compare the anticipated locations of cameras to the actual locations of cameras, scale bars were created using known stream measurements taken at the time of survey. As noted above, in an effort to test the repeatability of this research by an unspecialized user, the Rattlesnake Creek survey was carried out by a research assistant that followed the methodology used for the Deer Creek survey. The results for the Rattlesnake Creek and Deer Creek surveys are listed below.

4.1 Photo Alignment

The first consideration when importing images into Agisoft Metashape™ is photo alignment. For this study, the number of images that were aligned was influenced by the presence or absence of coded markers within each section. The absence of all markers from images created a large disparity between the total number of images and the number of images that were successfully aligned. The presence of markers produced diminishing returns once the number of markers exceeded 6 within each section. Table 7 below shows the relationship between number of markers and successful image alignment within Agisoft Metashape™.

Table 7. Deer Creek Run Image Count

Sensor	Number of Images	Aligned with Markers Present (0)	Aligned with Markers Present (3)	Aligned with Markers Present (6)	Aligned with Markers Present (12)
DSLR					
Section 1	41	18/41	38/41	41/41	41/41
Section 2	40	8/40	30/40	38/40	38/40
Section 3	33	16/33	33/33	33/33	33/33
iPhone					
Section 1	44	18/44	40/44	44/44	44/44
Section 2	30	8/30	22/30	28/30	30/30
Section 3	28	18/28	26/28	26/28	26/28
GoPro					
Section 1	18	13/18	18/18	18/18	18/18
Section 2	18	8/18	15/18	15/18	16/18
Section 3	18	10/18	18/18	18/18	18/18

4.2 Scale Creation

The purpose of photogrammetry is the creation of measurable structure from a moving or roving camera. That structure is created first by identifying keypoints in each photo, filtering those keypoints, registering those keypoints, projecting the intersection of those keypoints onto a 3D plane, and having those projections communicate with one another based on their relative location. Metashape™ automatically detects the locations of cameras and predicts where other projections, reprojections, and reconstructions of those projections should be. One way to make this process even more reliable is to implement coded markers into a survey, such as was done in this study. These markers are coded and printable from within the Metashape™ environment and

serve as keypoints in and between images. This is especially useful in areas like heavily vegetated streams where distinguishable features may be hard to identify.

While conducting the physical stream survey at the time of sampling, distances were measured between each marker. These distances were then imported into Metashape™ as known scalebars. These known scalebars provided the option to compare known measurements from the physical survey to the measurements that were being created via Metashape™. The known vs. expected measurements for Deer Creek sections are see in Figure 8 below.

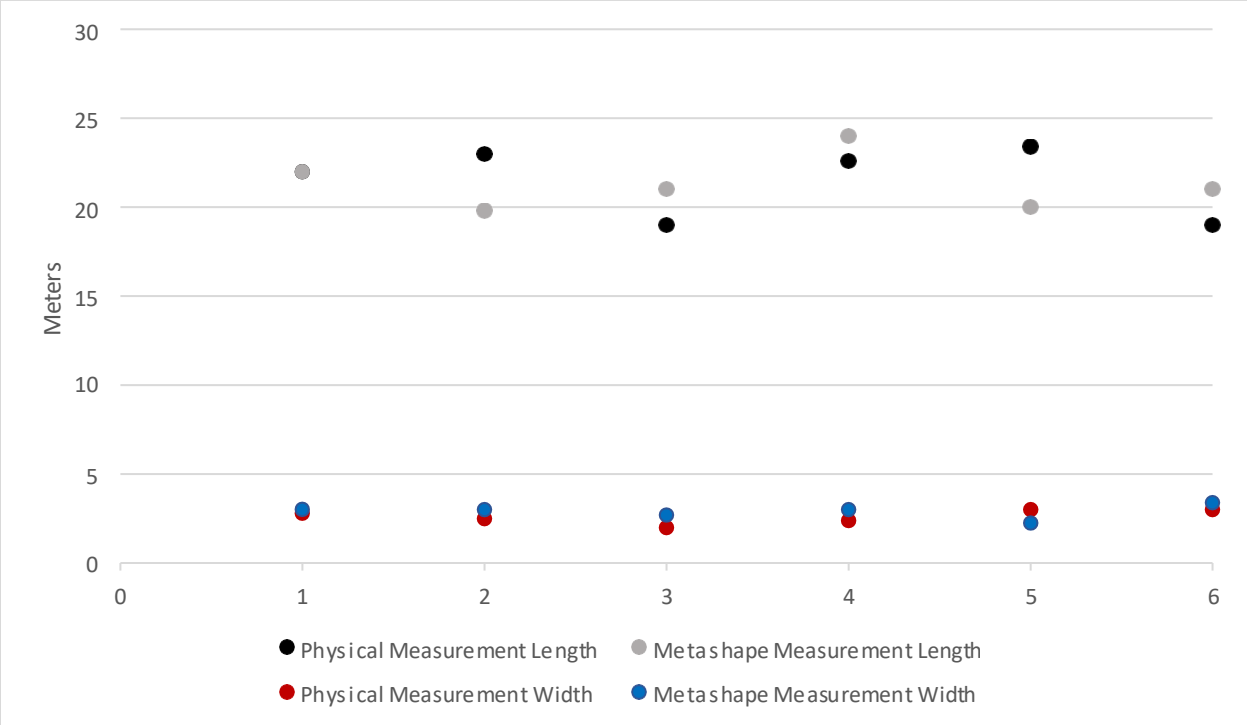

Figure 8. Physical Measurements vs Metashape™ Measurements from Deer Creek Runs. Note: Numbers 1 through 6 correspond to the following sections for both Deer Creek runs: 1 = Section 1 Run 1, 2 = Section 2 Run 1, 3 = Section 3 Run 1, 4 = Section 1 Run 2, 5 = Section 2 Run 2, 6 = Section 3 Run 2. (change section to S and run to R and then codify)

4.3 Gradual Selections

The purpose of the gradual selections of points within Agisoft Metashape™ is to remove bad matches between keypoints within the sparse and dense clouds. The results of this section build on the parameters utilized by the BLM for creating models of acceptable accuracy (Noble 2018). Metashape™ has four gradual selection methods: Image Count, Projection Accuracy, Reprojection Error, and Reconstruction Uncertainty; the latter three were tested and assessed by the RMSE and total keypoints removed for each camera along each section of Deer Creek. It is important to identify how many keypoints have been removed from each point cloud as the total number of keypoints serve as an indicator on overall model accuracy.

4.4 Projection Accuracy

Projection accuracy is the criterion that allows Metashape™ to filter out points within projections that were more poorly localized. Metashape™ saves an internal accuracy/scale value for each tie point of the correlation process. For example, Level 1 projection accuracy would mean that all points remaining in the cloud are correct projections from 2D to 3D space. The level corresponds to a set percentage, above which, a model becomes unreliable. In this study, that percentage was 90% of the total points meaning that level 2.2 selected 10% of the points in the cloud for removal before the next camera optimization step. The level corresponds to a set percentage, above which, a model becomes unreliable. Achieving a projection accuracy of 1 would mean a perfect model was created from the overlap between images. The projection accuracy level of 2.2 was used to eliminate those pixels which, due to either poor image overlap or noise within surrounding pixels, could not be matched below a level of 2.2.

Although level 1 would be ideal, it removed over 90% of the total points included in the model which eliminated the necessary amount for quality product creation.

Table 8. Images, Gradual Selection RMSE, and Number of Models by Section

Sensor	Number of Images	Reconstruction Uncertainty RMSE	Reprojection Error RMSE	Projection Accuracy RMSE	Number of 3D Models
DSLR					
Section 1	41	0.095	0.093	0.163	3
Section 2	40	0.09	0.089	0.133	3
Section 3	33	0.092	0.09	0.165	3
iPhone					
Section 1	44	0.102	0.095	0.2	3
Section 2	30	0.099	0.099	0.21	3
Section 3	28	0.106	0.107	0.448	3
GoPro					
Section 1	18	0.101	0.1	0.235	3
Section 2	18	0.086	0.085	0.106	3
Section 3	18	0.092	0.09	0.165	3

Figures 9, 10, and 11 below show the total points for Section 1 of Deer Creek after performing the gradual selections mentioned above. The trend in these errors for Section 1 was replicated in each of the other sections of the Deer Creek survey and in the Rattlesnake Creek survey.

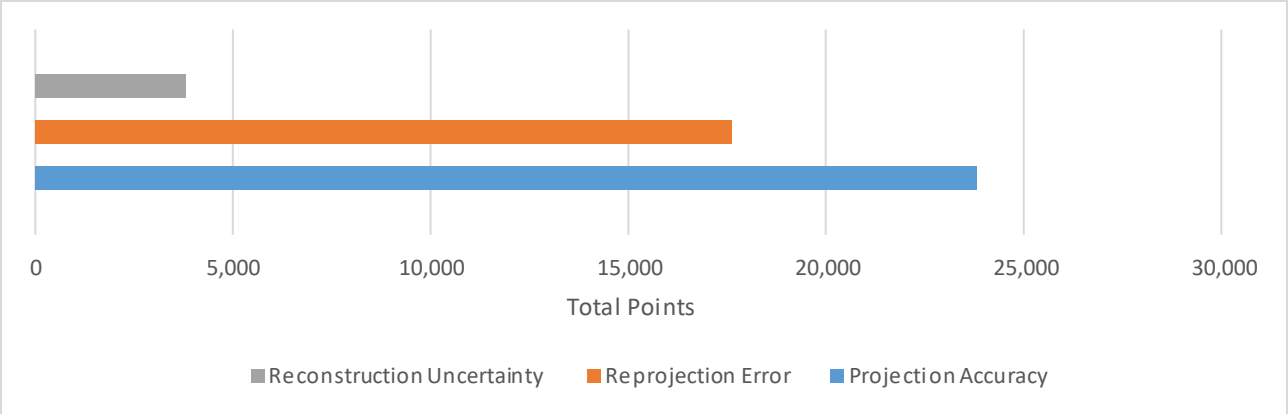

Figure 9. Section 1 DSLR Keypoint Totals (Deer Creek).

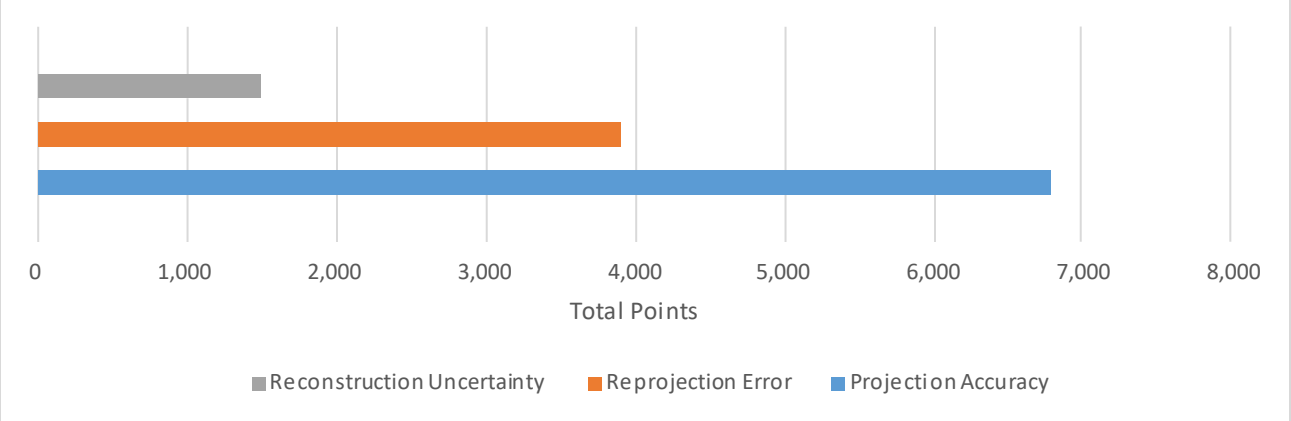

Figure 10. Section 1 GoPro Keypoint Totals (Deer Creek).

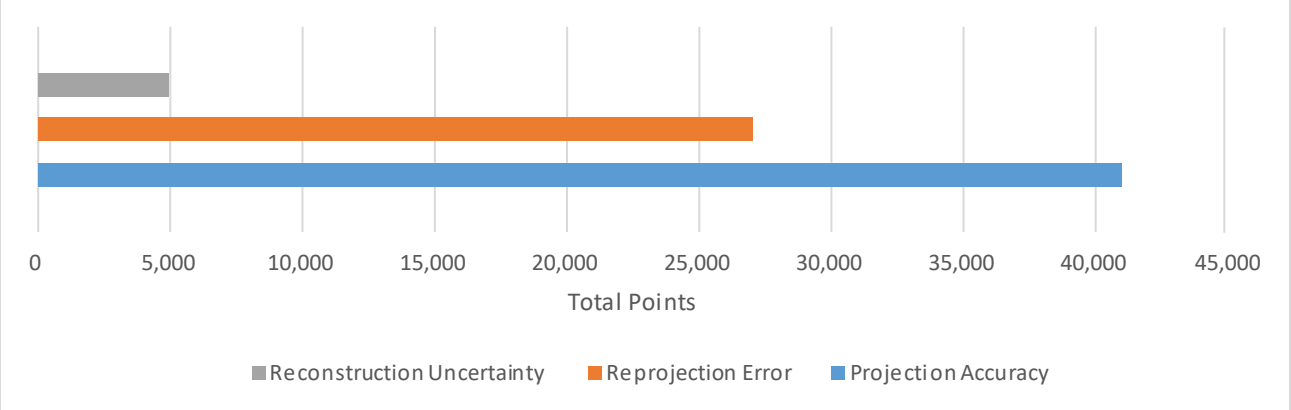

Figure 11. Section 1 Iphone Keypoint Totals (Deer Creek).

Figures 12 through 20 below show the RMSE for the gradual selection methods for each camera along each section of Deer Creek.

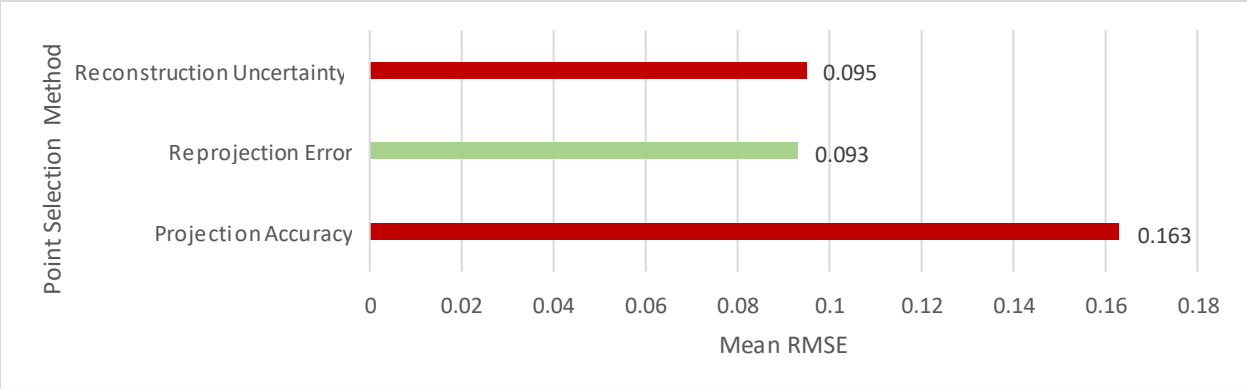

Figure 12. Gradual Selection RMSE DSLR Section 1 (Deer Creek).

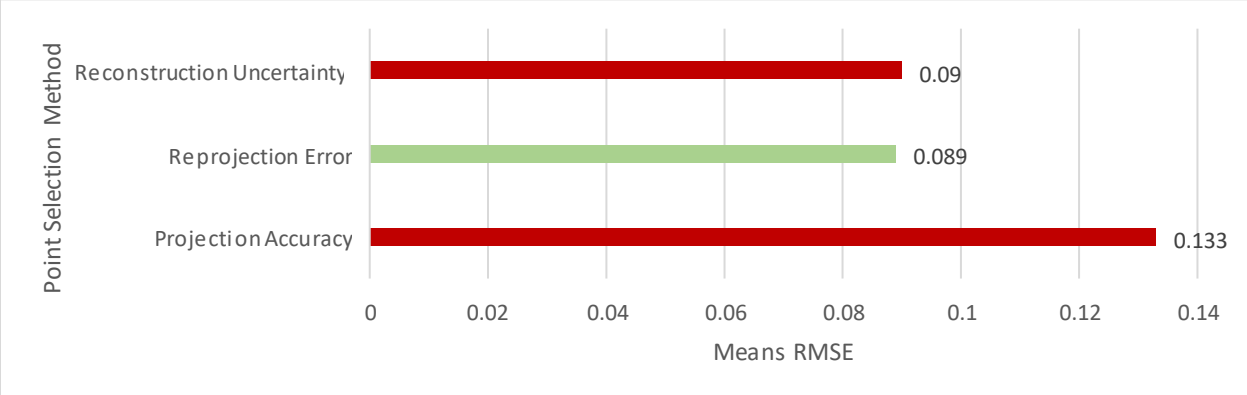

Figure 13. Gradual Selection RSME DSLR Section 2 (Deer Creek).

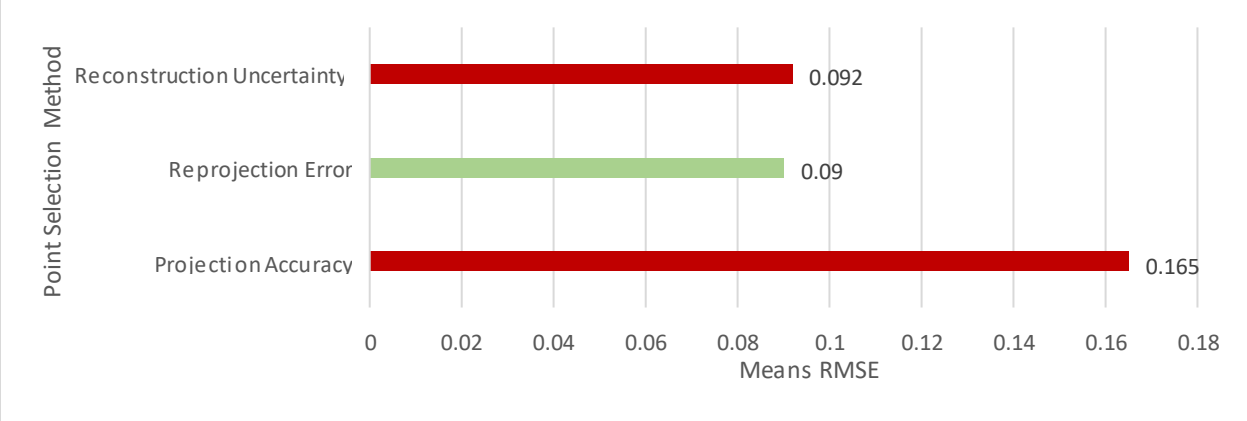

Figure 14. Gradual Selection RMSE DSLR Section 3 (Deer Creek).

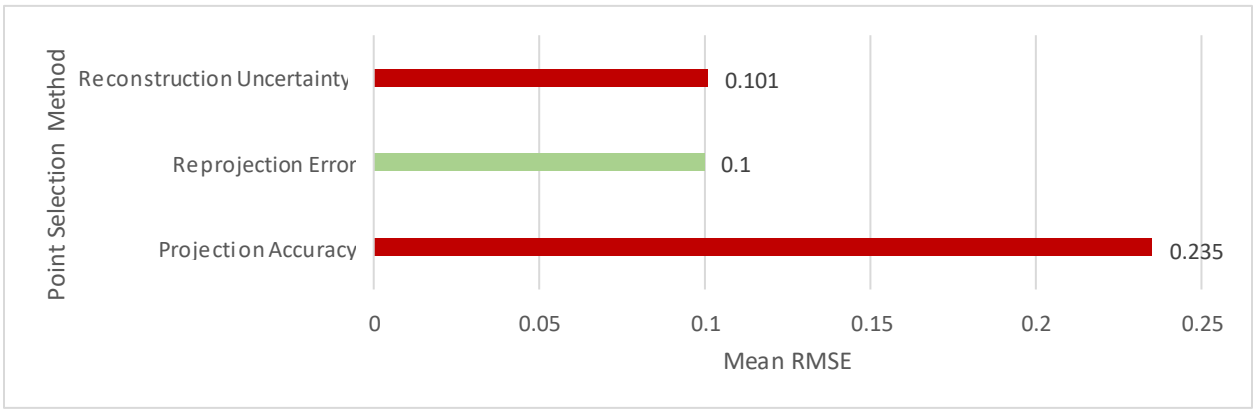

Figure 15. Gradual Selection RMSE GoPro Section 1 (Deer Creek).

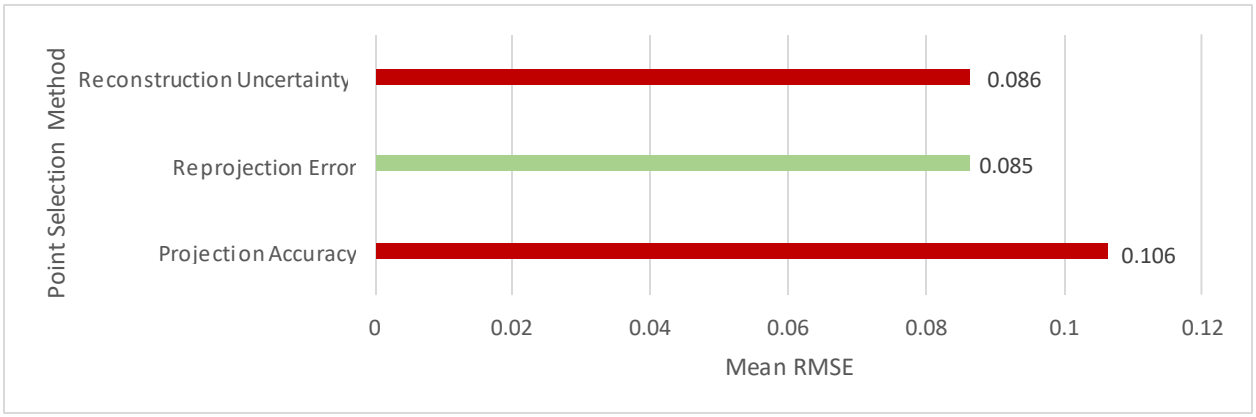

Figure 16. Gradual Selection RMSE GoPro Section 2 (Deer Creek).

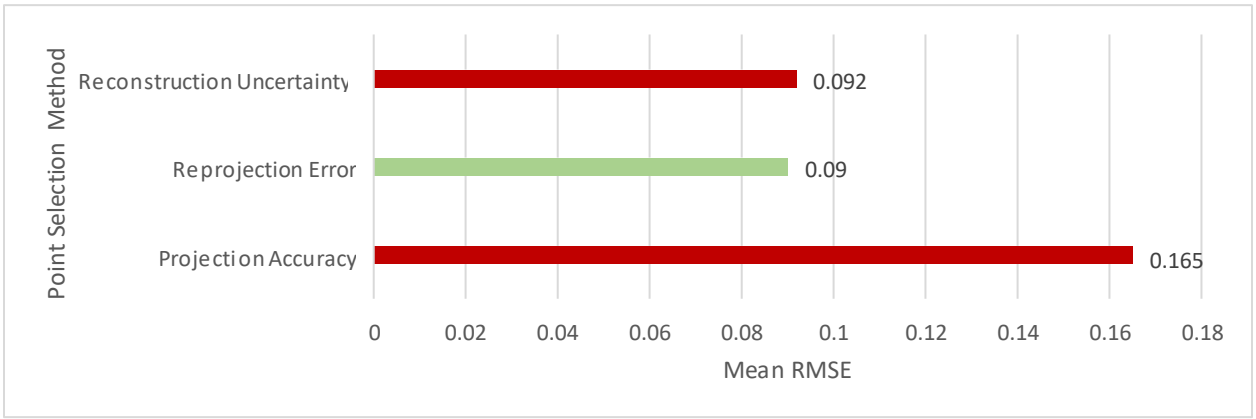

Figure 17. Gradual Selection RMSE GoPro Section 3 (Deer Creek).

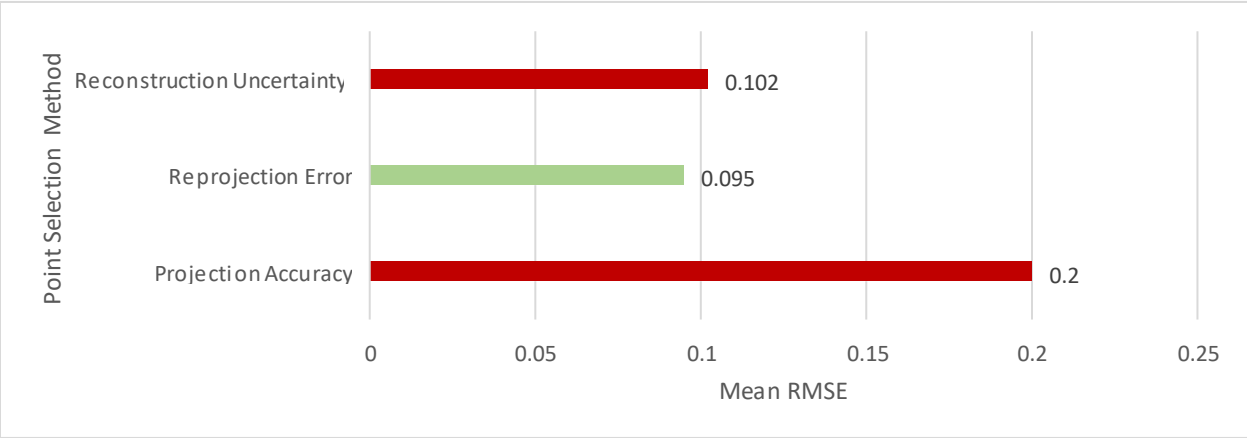

Figure 18. Gradual Selection RMSE iPhone Section 1 (Deer Creek)

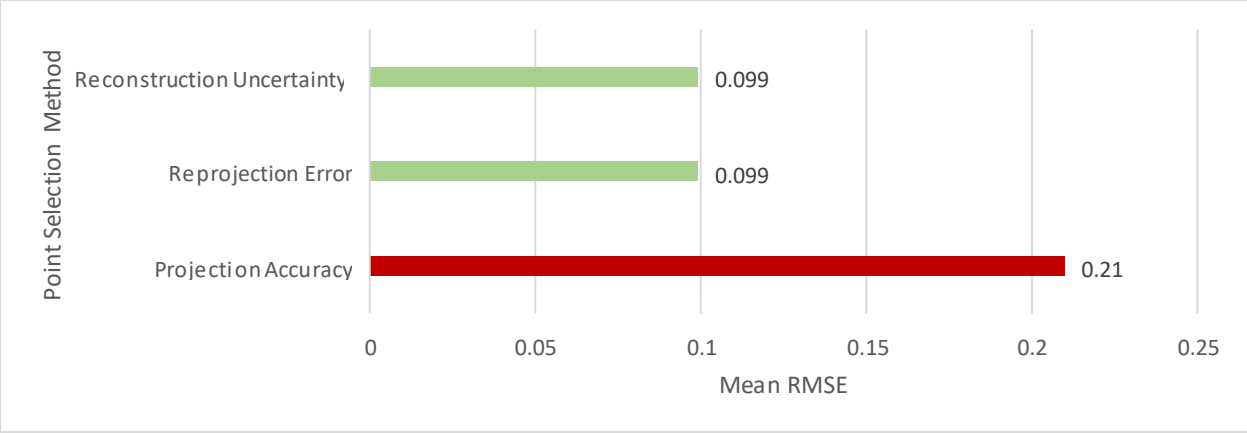

Figure 19. Gradual Selection RMSE iPhone Section 2 (Deer Creek).

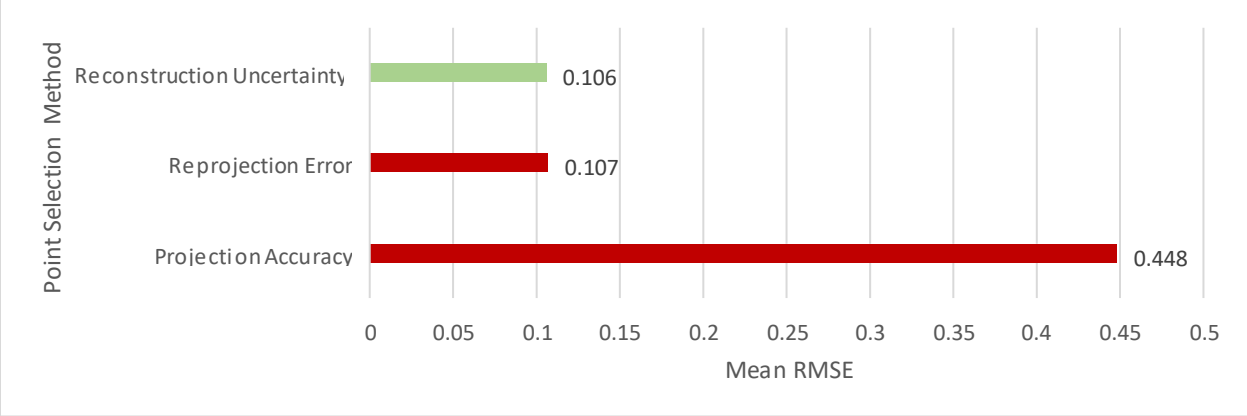

Figure 20. Gradual Selection RMSE iPhone Section 3 (Deer Creek).

4.5 Reprojection Error

Within Metashape™, the keypoints are referenced in three-dimensional space. The 3D point is the best fit of any given point that is matched on at least two photos. From that best fit 3D point, rays are reprojected back onto each two-dimensional photo. The difference between that 2D reprojected point and original 2D sub-pixel matched point is the reprojection error. For this study, a reprojection error of 0.2 pixels was used which means all valid keypoints that have been identified are removed if they are not accurate to at least the 0.2-pixel level. A simple way to think of pixels in terms of accuracy is with a 1 to 1 example. If spatial accuracy is guaranteed to 1 pixel, or has a RMSE of 1 pixel, this means that any pixel in an image would be within 1 meter of its 'true' location on the ground. For this study, all points were removed that were not within the 0.2-pixel range of their expected location given a known parameter.

4.6 Reconstruction Uncertainty

Reconstruction uncertainty deals with the accuracy of position points within the cloud. Similar to reprojection error, reconstruction uncertainty takes the intersection of two rays and identifies a direction in which the variation for that point position is at a maximum and a minimum. These minimum and maximum values are divided and a level of uncertainty is assigned to each point within a dense or sparse point cloud.

Similar to projection accuracy, a level 1 reconstruction uncertainty would mean the position of each point within a point cloud is 100% correct. Therefore, the lower the level the more accurate the model. This selection removed the most points in this study, and a level of 100 was the lowest reconstruction uncertainty that could be attained without removing over 90% of each dense point cloud. The large amount of vegetation present in each image created a significant amount of uncertainty when attempting to reconstruct a model.

This aligns with the results outlined by previous studies where a Leaf Area Index of over 50% creates significant variance in model reconstruction (Duke 2018).

4.7 Deer Creek Physical Survey

The purpose of collecting physical stream data while testing each camera on each section of stream was to have reliable measurements that could be used to validate the measurements coming from Metashape™, and to create qualitative data similar to the information collected during traditional stream surveys. Table 9 shows all of the data from the two sampling dates on Deer Creek, as well as the total time each survey took for both the lab and field components.

Table 9: Deer Creek Runs 1 and 2 Sampling Data

7/7/2020	Deer Creek	Length	WettedWidth	Depth	Large Woody Debris Present	Riaprian Vegetation Classification	Streamback Substrate Size	Estimated Vegetative Cover	Bank Incision Present
Physical Stream Survey	Section1	22 meters	2.8 meters	22.86 centimeters	N	Mustards, clovers, sedge grass, bull thistle, spruce	Gravel	>95%	N
Metashape™ Measurements		22 meters	3.02 meters	N/A					
Physical Stream Survey	Section2	23 meters	2.5 meters	25.4 centimeters	N	Willow, mustards, sedge grass, wild rose	Cobble	>95%	Y
Metashape™ Measurements		19.8 meters	3 meters	N/A					
Physical Stream Survey	Section3	19 meters	2 meters	30.48 centimeters	Y	Clover, common hops, mustards, willows	Sand-Cobble	<85%	Y
Metashape™ Measurements		21 meters	2.7 meters	N/A					
Total Lab Time	12 hours								
Total Stream Survey Time	3.5 hours								
Total Working Hours	15.5 hours								

8/8/2020	Deer Creek	Length	WettedWidth	Depth	Large Woody Debris Present	Riaprian Vegetation Classification	Streamback Substrate Size	Estimated Vegetative Cover	Bank Incision Present
Physical Stream Survey	Section1	22.6 meters	2.4 meters	17.78 centimeters	N	Mustards, clovers, sedge grass, bull thistle, spruce	Gravel	>95%	N
Metashape™ Measurements		24 meters	3 meters	N/A					
Physical Stream Survey	Section2	23.4 meters	2.25 meters	17.78 centimeters	N	Willow, mustards, sedge grass, wild rose	Cobble	>95%	Y
Metashape™ Measurements		20 meters	3 meters						
Physical Stream Survey	Section3	19 meters	2 meters	27.94 centimeters	Y	Clover, common hops, mustards, willows	Sand-Cobble	<90%	Y
Metashape™ Measurements		21 meters	3 meters	N/A					
Total Lab Time	12 hours								
Total Stream Survey Time	3.5 hours								
Total Working Hours	15.5 hours								

4.8 Rattlesnake Creek Physical Survey

One survey was completed on Rattlesnake Creek by a research assistant in an effort to test the applicability of the methodology by an unspecialized user.

The research assistant received minimal training on plant/tree identification and visual vegetation estimation. They were provided a list of procedures and selection parameters and instructed to carry out the survey to the best of their ability. Table 10 shows the data from the one sample conducted along Rattlesnake Creek, complete with the Metashape™ measurements that were estimated via the scale bar creation and gradual selection workflows.

Table 10: Rattlesnake Creek Run Sampling Data

1/24/2021	Rattlesnake Creek	Length	WettedWidth	Depth	Large Woody Debris Present	Riaprian Vegetation Classification	Streamback Substrate Size	Estimated Vegetative Cover	Bank Incision Present	18	3.75
Physical Stream Survey	Section 1	17 meters	3.4 meters	8 inches	N	Dead grass and deciduous trees	Cobble	<60%	N		
Metashape™ Measurements		18 meters	3.75 meters	N/A							
Total Lab Time	3.5 hours										
Total Stream Survey Time	1 hour										
Total Working Hours	4.5 hours										

There will always be expected variability when gathering stream data such as wetted widths and total stream lengths, but the results from Table 10 show the length of the section is accurate to 1 meter and the average wetted width is accurate down to 35 cm.

4.9 Metashape™ Products

Once the image processing, scalebar creation, and coordinate system workflows were completed within Metashape™, the dense point cloud could be transformed into a DEM, Orthomosaic, and a textured mesh or 3D model of the stream. The stream channel measurements (i.e., transect length, average depth, average width) were taken from the 3D meshes created within Metashape™. The DEMs and Orthomosaic products were also used to compare changes in stream bank and channel configurations. Based on the two Deer Creek Runs, Metashape™ has the ability to estimate changes in width and depth over a 30-day period when flows were declining. This translates to a potential for Metashape™ to provide measurements on changes in stream bank and channel configuration that may occur due to high flow events on streams with heavy vegetation during different times of year. Figures 21 through 26 below show the textured meshes created within Agisoft Metashape™ complete with measured distances used to determine the wetted widths for each section. Part 2 shows how the meshes can be navigated and measured at different points within the software. These models were created for each section of both the Deer Creek runs and the Rattlesnake Creek run. Figures 21 through 26 are included to show the 3D navigation capabilities within Metashape™ which provides potential benefits if interested in calculating leaf area index or volumetric measurements of vegetation along stream banks.

Figure 21. 3D Model Section 1 iPhone Camera

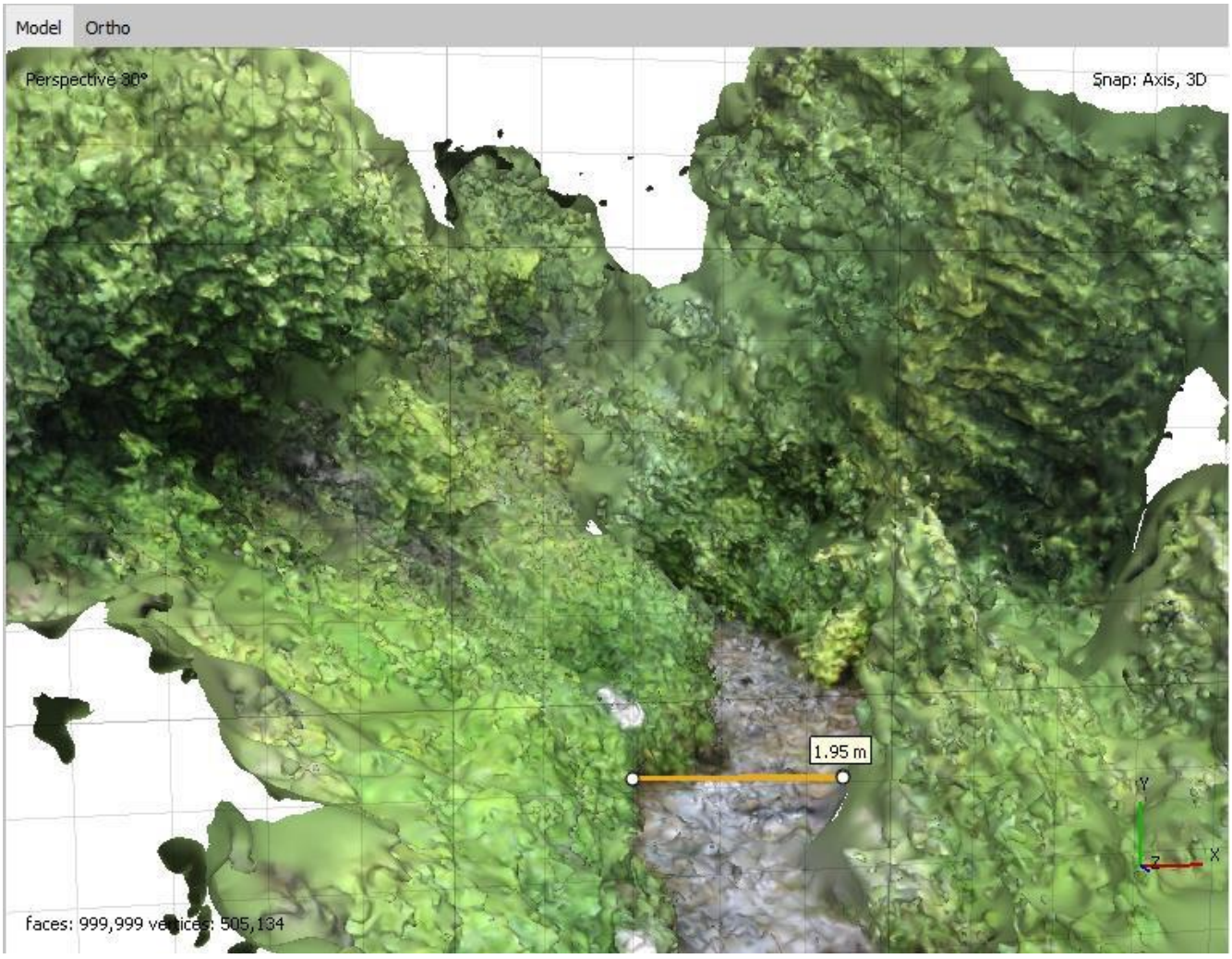

Figure 22. 3D Model Section 1 iPhone Camera Part 2

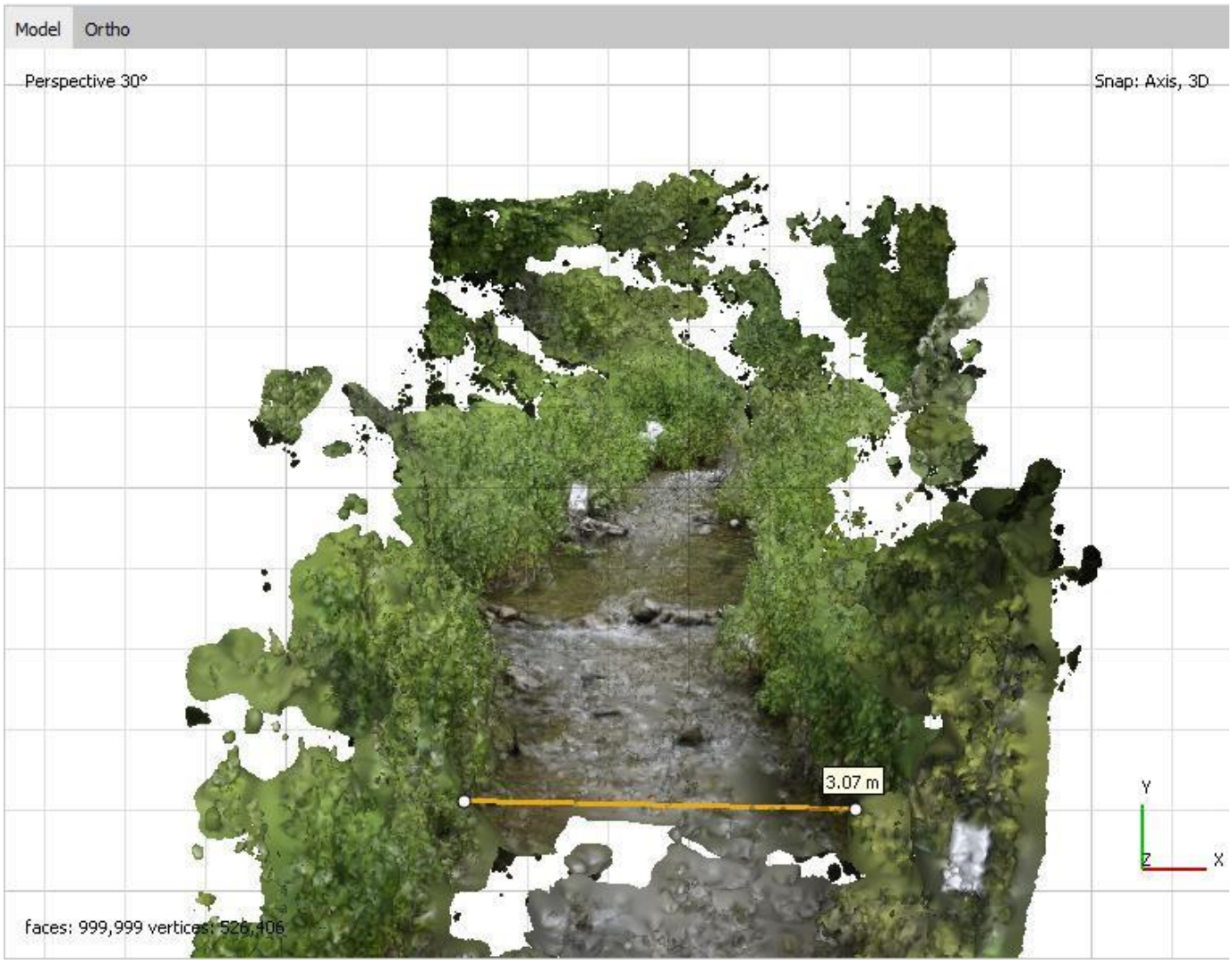

Figure 23. 3D Model Section 1 DSLR Camera

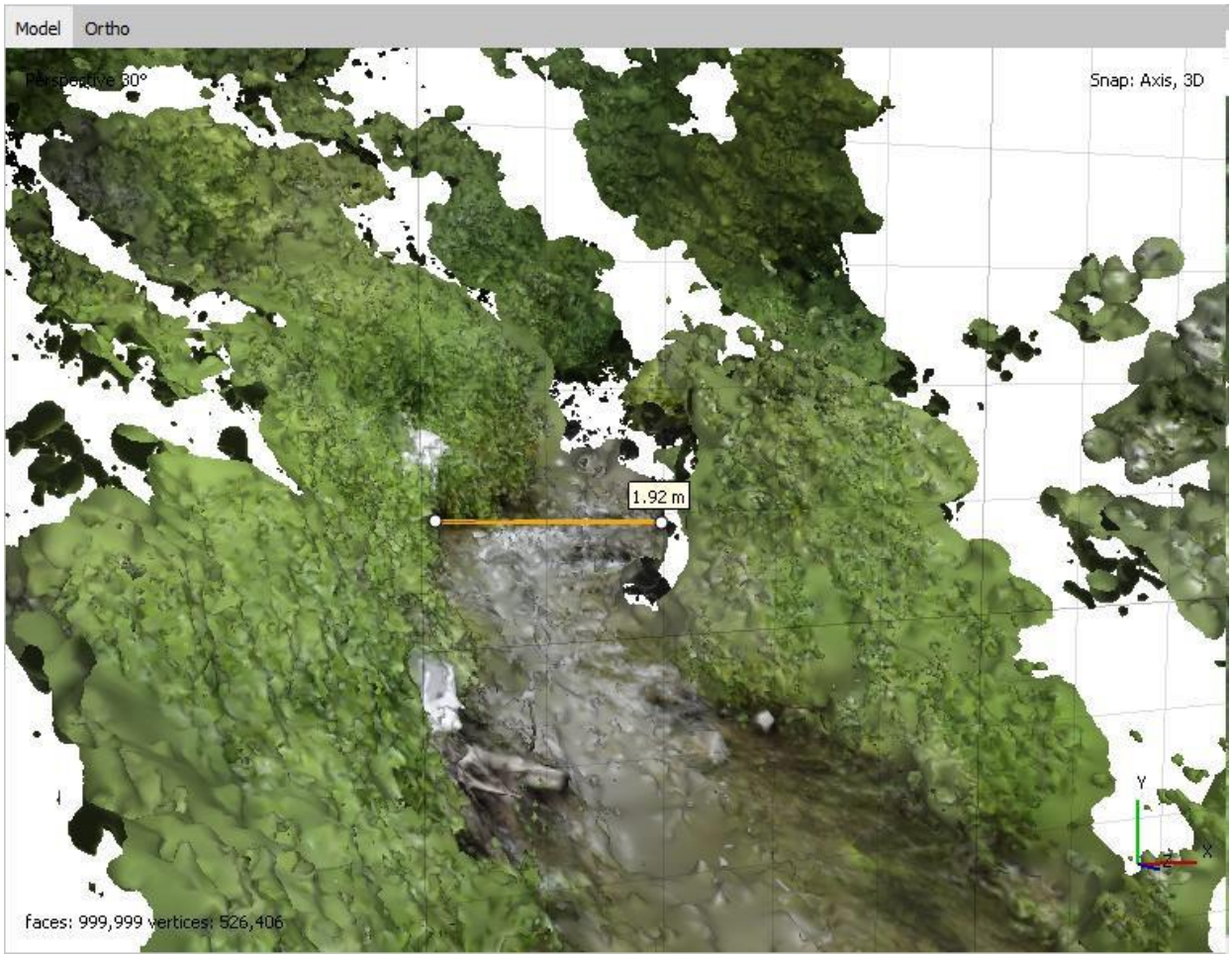

Figure 24. 3D Model Section 1 DSLR Camera Part 2

Figure 25. 3D Model Section 1 GoPro Camera

Figure 26. 3D Model Section 1 GoPro Camera Part 2

5. Discussion

There has been a sharp rise over the past two decades in the application of photogrammetry in a wide range of scientific fields including agriculture, geomorphology, and history because of the amount of data that can be collected and analyzed over a relatively short period of time (Dietrich 2016). Broad, workflow-based, photogrammetric studies have been carried out to better understand how the SFM-MVS processes work within different software programs (M.R. James and Robson 2012). Smaller scale studies gave been carried out to determine the impact of factors like vegetation and image count on overall 3D model accuracy (Duke 2018). Although a broad understanding of SFM-MVS processes is important, and controlled studies are crucial in determining the impacts of variables like vegetation, ambient lighting, and camera parameters on 3D model creation, the purpose of this study was to explore the efficacy of using Capture to produce quantitative and qualitative data along heavily vegetated streams where other remote sensing options are either impossible or prohibitively expensive.

The results from this study demonstrate that Capture is capable of producing, locally coordinated 3D models within Agisoft Metashape™ using the three types of hand-held cameras tested in this study. The application of Capture provided similar results in comparison to the stream geometry measurements taken during the Deer Creek and Rattlesnake Creek surveys. The ability to create photogrammetric models of Deer Creek and Rattlesnake Creek proved successful without the need for georeferencing. Capture can be applied to many disciplines that require making physical measurements in areas with variable vegetation and lighting without a significant time investment or the need for expensive camera or GPS equipment.

5.1 Most Suitable Camera

The results from the gradual selections carried out within Agisoft Metashape™ indicate that the projection accuracy and reprojection error for all models of Deer Creek and Rattlesnake Creek were within acceptable RMSE thresholds without removing too much of the point cloud for the model to still be viable. The reconstruction uncertainty of each model was too high to be considered a viable option for measurement as over 90% of the total points in each section's dense cloud were removed to achieve an acceptable RMSE. This is not surprising as the high amount of vegetation included in each image made reconstructing those images near impossible. The impact of vegetation on photogrammetry is well documented, and this study attempted to solve that issue by increasing the number of images taken of each section (Duke 2018). However, increasing the number of images taken did not prove to be enough to remedy the issues caused by heavy vegetation. The only camera capable of producing a model that fit within the reconstruction uncertainty parameters was the Sony a6500 (DSLR) because of the high number of points present in the dense cloud. However, the measurements taken from the models that adhered to the reconstruction uncertainty RMSE threshold were not noticeably more accurate than the measurements taken from the models that did not adhere to the reconstruction uncertainty RMSE threshold. Even though an acceptable reconstruction uncertainty could not be achieved for each model, the number of points that remained after the projection accuracy selection of level 2.2 and reprojection error selection of 0.2 pixels meant that the models could still be used for measurement. Thus, reconstruction uncertainty was not deemed to be a significant determinant of accurate models within Agisoft Metashape™ when employing Capture along heavily vegetated streams.

The importance of coded markers cannot be overstated when capturing images with hand-held cameras along heavily vegetated streams. This is especially true when models will not be georeferenced to a real-world coordinate system, but be left in the localized coordinate system created within Agisoft Metashape™. As seen with the high point removal during reconstruction uncertainty, the amount of vegetation on the periphery of the stream makes image matching quite difficult. This fact was further validated by the number of misaligned images during the photo alignment phase in Agisoft Metashape™ when 0 markers were present during the survey. Interestingly enough, the number of aligned photos did not increase in a meaningful way when at least 3 markers were placed in each section. This proved very useful as the amount of time it took to place 12 individual targets within a 22-meter stretch of stream and then retrieve and replace them in the next section was quite high. Additionally, the placement of at least three markers meant at least three scale bars could be created for each section of stream.

The results indicate that all hand-held cameras included in this study are capable of producing accurate models within heavily vegetated environments. The measured vs. expected locations of markers within each image combined with the low RMSE achieved with the reprojection error threshold of 0.2 pixels for each camera shows that higher megapixel cameras do not produce significantly more accurate models within Agisoft Metashape™. In fact, the models with the most accurate measurement between what was measured at the time of survey and what was produced via Agisoft Metashape™ were created from the iPhone camera's images. Therefore, the most appropriate sensor for employing Capture along heavily vegetated streams is the iPhone camera, as it produced similar quality models and is the most ubiquitous camera of the three tested in this study.

If researchers are looking for highly accurate point clouds with an abundance of points for rigorous point selections, then a DSLR camera with at least 24 MP is best. If researchers are looking for the best models with the fewest images required, then a GoPro or similar camera with a fisheye lens would be best.

5.2 Image Processing Workflow

The results from the gradual selection methods and the image processing workflows indicate that the steps being implemented by the USGS are fitting using aerial photos or when acquiring many images from around stationary objects in conjunction with accurate GPS data. For this study, the USGS workflow was amended to include the merging of multiple Chunks and the implementation of markers within Agisoft Metashape™ in order to compare changes between 3D models without the need for georeferencing. Had accurate GPS data been collected for each image at the time of survey, then change over time comparisons could be made in the future as long as similar, or more accurate georeferencing steps occurred. However, the results from this study show that importing the local reference information from one point cloud into a separate Chunk within the same workspace creates the ability for local coordinate comparison. Figures 21 through 26 show the relationship between quantitative measurements when moving through the 3D models of Section 1. This pattern continued through all three sections and showed similar results when comparing merged chunks for each section. This could prove quite useful when assessing the efficacy of river restoration efforts along heavily vegetated streams because it could provide a more standardized means of tracking change over time without the need for georeferenced imagery.

5.3 Capture Measurements

The results from this study show that the 3D models produced from images taken with an iPhone camera provide measurements that are close to the physically measured stream characteristics. They complement the image processing workflows currently being used by the USGS for photogrammetry studies, and provide additional steps for creating locally coordinated models for comparison. The physical measurements taken of the stream at the time of survey not only provide quantitative information, but are tied to a 3D model which serves as a navigable 'snapshot' of the stream at the time of survey which could be used for future comparison.

The lab and field effort results from Tables 9 and 10 indicate that Capture collection, image post processing, and model creation and comparison is a relatively quick process that doesn't require much specialization. Additionally, the results show a significant reduction in both field and lab component times after the first Deer Creek survey was complete. The workflows and results presented in this study can be followed and replicated to provide the measurements obtained herein as well as measurements of instream habitat (i.e., pools, riffles, etc.) and large woody debris as long as an individual or organization has access to Agisoft Metashape™.

Finally, Table 11 below shows the relative cost for purchase of a professional license for Agisoft Metashape™ compared to costs for two of the other most prominent software programs used for 3D model creation and comparison.

Table 11: Professional License Fee Structure for Comparable Photogrammetry Programs

	Annual Fee	One-Time Fee
Agisoft Metashape™	N/A	$499.00
DroneMapper	N/A	$999.00
Pix4D	$3,000	N/A

Agisoft Metashape™ is clearly the most affordable of these three programs and has all of the capabilities necessary for comprehensive 3D analysis without the need for georeferenced imagery.

5.4 Constraints

The results from the reconstruction uncertainty gradual selections indicates that these models cannot be considered highly accurate. The angle from which the images were taken combined with the heavy amount of vegetation in each image makes the uncertainty of reconstruction too high. This means that the models would never serve well as stand-alone products, but rather as a complimentary tool to traditional stream surveys.

Another constraint of Capture along heavily vegetated streams is its inability to provide accurate riparian vegetation data. One of the initial purposes of this research was to remedy the issues inherent to visual estimation and the subsequent comparison of vegetation types and vegetation densities within riparian zones. Unfortunately, the study design proposed herein was unable to produce models that could accurately identify anything outside of the stream corridor. Although vegetation can clearly be seen outside of the stream corridor it is impossible to differentiate between various types of vegetation and approximate overall vegetative cover as the reconstruction uncertainty is too high using hand-held cameras.

An important consideration regarding image acquisition in the field relates to the internal filtering that occurs when capturing images with a sensor that automatically employs internal filtering with preferred ISO, aperture, and focus depending on conditions resulting from resolutions, wind, and solar angles. The iPhone and GoPro sensors differ from the Sony DSLR camera used in this study in that the iPhone and GoPro sensors automatically determine the best internal settings based on changes in objects of interest (e.g., moving vegetation resulting from wind, reflectivity from changing solar angles, distance to objects). The preferred setting for field sampling, considering the autocorrected internal parameters for the aforementioned sensors, would be consistent lighting, minimal wind, and similar distance to object (s) of interest (e.g., placed scale markers, vegetation, in stream habitats, etc.). In an effort to optimize sampling, increasing the number of images taken on an overcast, calm, day would be best for image acquisition which highlights another constraint of this research.

Another constraint highlighted by the results of this study is future model comparison. For example, when evaluating the accuracy of a DEM, a comparison is typically made between the georeferenced DEM and a differential GPS survey to determine the error between what the model displayed and what was measured with the differential GPS. Because no differential GPS data were collected in this study, the accuracy of the models can only be compared within local coordinate space meaning future comparisons have to happen within the same software program or a software program that can compare models within an arbitrary coordinate system. The models cannot be exported as DEMs for use in another program like ArcGIS Pro unless they have accompanying spatial data. This highlights the last constraint of this study which is software preference and use. All of the model creation and comparison

occurred within Agisoft Metashape™. This study is not repeatable unless a user has access to that software program. The principles for image acquisition and study design would most assuredly translate to other studies that choose to use another program, but certain parameters may not translate to other programs like Pix4D and Drone Mapper. Lastly, there is anopen source free-wareoption for Drone Mapper, but this requires a degree of specialization which veers from the intent of this study. If a user possessed some coding ability they would be able to utilize the Open Drone Mapper program without paying the one-time fee presented in Table 11 above.

The constraints mentioned above could be addressed in another study by simply employing a dGPS survey and expanding the comprehensive workflows outlined in this study to another software program. By expanding the study in these ways, one could determine the impact that some of the 'black-box' algorithms used in image processing, key-point identification, and feature matching have on overall model creation and create the opportunity for DEM comparisons in any GIS software program. Other smaller-scale studies might choose to focus on errors created in DEMs as a result of shading, camera height, and vegetation in an effort to further standardize the models produced herein. However, the capabilities of Capture outlined in this study make it a useful tool for complementing traditional stream surveys on small streams in western Montana or elsewhere.

An avenue worth pursuing in future studies would be the use of embedded GPS data in the EXIF info included in each image taken by the iPhone camera. The GPS accuracy for each image varies depending on cell tower location and service provider, but a logical next step for future studies would be incorporating the appurtenant GPS data into the 3D models to establish known geographic locations for each model which would allow for DEM comparison and

registration within other GIS programs like Global Mapper and ArcGIS. This study did not attempt to remedy this constraint because one of the questions posed herein focused on the capability of each sensor to produce models of similar accuracy; including native GPS data from the only sensor capable of producing such information could have potentially skewed the model accuracy in favor, or against, the iPhone, and thus, was intentionally left out. It is worth noting here that this study found the iPhone camera capable of producing 3D models with comparable accuracy to both GoPro and DSLR cameras, answering question 1 posed in this study, so the constraint of 'real world' model comparison could potentially be addressed by employing known GPS data inherent to a GPS capable camera.

The final constraint worth noting relates to water depth measurements. It is currently impossible to gather water depth information solely from images or 3D models. This is a constraint inherent to photogrammetry in general. Although the intention of this research was to test the ability of the models to create objective measurement, the only way gather water depth information is through 3D model comparison using wetted width measurements and noting change in depth. This measurement, along with vegetation classification and vegetative percent cover, were part of the physical measurements mentioned in Table 2 above. These measurements, among others were collected at the time of image acquisition survey. Future studies should explore the potential to calculate these measurements by utilizing real world coordinate systems for change comparisons.

6. Conclusion

The key takeaways from this study are that cell phone cameras capable of taking RAW formatted imagery can be used to produce accurate wetted width and stream section measurements within Agisoft Metashape™, that scale markers must be used to compare software

measurements to physical measurements when not employing dGPS corrected keypoints, and that Capture can complement physical stream surveys along heavily vegetated streams between orders 1 and 3 (Strahler 1952). The benefit to using Capture as a complementary tool instead of simply employing repeat photography is twofold. First, there is no need to take photos from the exact same location during each survey thanks to the photogrammetric principles that perform camera position corrections within Agisoft Metashape™. This means that surveyors can go to a section of stream and simply take photos as they walk within the stream corridor even if they begin from a slightly different location or perspective than the previous survey. This also means that scale marker locations do not have to be in the same location as their placement can be arbitrary as long as at least two markers can be seen from each image. Second, the models created via Capture are 3D 'snapshots' of the stream at the time of survey. These 3D models have advantages over 2D representations of stream corridors as they can be viewed from various angles and perspectives. This creates the opportunity for more specialized stream technicians to lay eyes on a particular section of stream even if they were not there at the time of survey. The ability for relatively untrained stream technicians to gather data along a section of stream and provide a navigable 3D model to more specialized technicians is an invaluable opportunity when it comes to measuring the efficacy of stream restoration efforts along streams where other remote sensing options like drone imagery or LiDAR scans are either impossible due to heavy vegetation or prohibitively expensive. Lastly, it is worth noting that the applications for capture extend to other areas outside of stream corridors. The workflows provided in this study could be applied along trails, river access points, landscape restoration and/or design applications, and documentation of various other phenomena using change over time comparisons.

7. References

Abel-Aziz, Y.I. and H.M. Karara. 1971. Direct Linear Transformation from Comparator Coordinates Into Object Space Coordinates. *American Society of Photogrammetry* 1: 11-18.

Angeler, D.G. and C.R. Allen. 2016. Quantifying resilience. *Applied Ecology* 53(3): 617 – 624.

Armistead, C.C. 2013. Applications of Structure from Motion Photogrammetry to River Channel Change Studies. PhD thesis, Boston College. College of Arts and Sciences.

American Society for Photogrammetry and Remote Sensing. 2016. Manual of Photogrammetry. 6.

Bangen, S.G., J.M. Wheaton, N. Bouwes, B. Bouwes, and C. Jordan. 2014. A methodological intercomparison of topographic survey techniques for characterizing wadeable streams and rivers. *Geomorphology* 206: 343 – 361.

Brasington, J., B.T. Rumsby, and R.A. McVey. 2000. Terrestrial laser scanning and digital photogrammetry techniques to monitor landslide bodies. *International Archives of Photogrammetry, Remote Sensing and Spatial Information Science* 35(Part B5): 246 – 251.

Baumberg, A. 2000. Reliable feature matching across widely separated views. *Proceedings of the IEEE Conference on Computer Vision and Patter Recognition* 1: 774 – 781.

Bernhardt, E.S., M.A. Palmer, G. Allan, K. Alexander, S. Barnas, J. Brooks, S. Carr, C. Clayton, J. Dahm, and Follstad-Shah, et al. 2005. Synthesizing US river restoration efforts *Science* 308 (5722): 636 – 637.

Bird, S., D. Hogan, and J. Schwab. 2010. Photogrammetric monitoring of small streams under a riparian forest canopy. *Earth Surface Processes and Landforms* 35: 952 – 970.

Brown, D.C. 1971. Close-Range Camera Calibration. *Photogrammetric Engineerin*g 37(8): 855–866.

Cao, F., F. Guichard, and H. Hornung. 2010. Information capacity: a measure of potential image quality of a digital camera. *Proceedings of the Society of Photo-Optical Instrumentation Engineers* 1: 17 – 18.

Capon, S.J., L.E. Chambers, R. MacNally, R.J. Naiman, P. Davies, N. Marshal, J. Pittock, M. Reid, T. Capon, M. Douglas, J. Catford, D.S. Baldwin, M. Stewardson, J. Roberts, M. Parsons, and S.W. Williams. 2013. Riparian Ecosystems in the 21st century: hotspots for climate change adaptation? *Ecosystems* 16: 359-381.

Carrivick, J.L., M.W. Smith, and D.J. Quincey. 2016 *Structure from Motion in the Geosciences*, Oxford: John Wiley & Sons, Ltd.

Chandler, J., and J. Fryer. 2013. AutoDesk 123D Catch – How accurate is it? *Geomatics World* 28 – 30.

Conniff, R. 2014. Rebuilding the natural world: A shift in ecological restoration. *Yale Environment 360*.

Dietrich,W.E. 1987. Mechanics of flow and sediment transport in river bends. *River channels: environment and process* 18: 179–227.

Dietrich, J.T. 2016. Riverscape mapping with helicopter-based structure-from-motion photogrammetry. *Geomorphology* 252: 144 -157.

Duke, C. 2018. Evaluation of Photogrammetry at Different Scales. MS thesis, Auburn University. Soil and Environmental Sciences.

Fonstand, M.A., J.T. Dietrich, B.C. Courville, J.L. Jensen, and P.E. Carbonneau. 2013. Topographic Structure from Motion: a new development in photogrammetric measurement. *Earth Surface Processes and Landforms* 38: 421-430.

Furukawa, Y., and J. Ponce. 2009. Carved visual hulls for image-based modelling. *International Journal of Computer Vision* 81: 53 – 67.

Gallay, M. 2013. Section 2.1.4: direct acquisition of data: airborne laser scanning. *Geomorphological Techniques (Online Edition)*. London: British Society for Geomorphology.

Gienko, G.A., and J.P. Terry. 2014. Three-dimensional modeling of coastal boulders using multi-view image measurements. *Earth Surface Processes and Landforms* 39(7): 853 – 864.

Gloss., and E.S. Bernhardt. 2007. River and riparian restoration in the southwest: Results of the national river restoration science synthesis project. *Restoration Ecology* 15(3): 550 - 562.

Granshaw, S.I. 1980. Bundle adjustment methods in engineering photogrammetry. *The Photogrammetric Record* 10: 181-207.

Gregory, S.V., F.J. Swanson, W.A. McKee, and K.W. Cummins. 1991. An ecosystem perspective of riparian zones. *BioScience* 41(8): 540-551.

Gruen, A. 2012. Development and status of image matching photogrammetry. *The Photogrammetric Record* 27(137): 36 – 57.

Hansen Lotic Assessment. 2020. U.S. Lotic Wetland Ecological Health Assessment for Streams and Small Rivers. http://www.ecologicalsolutionsgroup.com/Documents/PDFforms/UserManuals/USALoticSurveyManual.pdf (last accessed 8 February 2021).

Horton, R.E. 1945. Erosional development of streams and their drainage basins: hydrophysical approach to quantitative morphology. *Bulletin of the Geological Society of America* 56(3): 275–370.

Husson, E., F. Lindgren, and F. Ecke. 2014. Assessing biomass and metal contents in riparian vegetation along a pollution gradient using an unmanned aircraft system. *Water Air Soil Pollution* 225: 1957.

James, M.R., and S. Robson. 2012. Straightforward reconstruction of 3D surfaces and topography with a camera: Accuracy and geoscience application. *Journal of Geophysical Research: Earth Surfact* 117(3).

Kennedy, R.E., S. Andrefouet, and W.B. Cohen. 2014. Bringing an ecological view of change to Landsat-based remote sensing. *Frontiers in Ecology and the Environment* 12(6): 339 – 346.

Kenefick, J.F., M.S. Gyer, and B.F. Harp. 1972. Analytical self-calibration. *Photogrammetric Engineering and Remote Sensing* 38: 1117 -1126.

Lambin, E.F., B.L. Tuner, H.J. Geist, S.B. Agbola, A. Angelse, J.W. Bruce, O.T. Coomes, R. Dirzo, G. Fischer, C. Folk, P.S. George, K. Homewood, J. Imbernon, R. Leemans, X. Li, E.F. Moran, M. Mortimore, P.S. Ramakrishnan, J.F. Richards, H. Skanes, W. Steffen, G.D. Stone, U. Svedin, T.A. Veldkamp, C. Vogel, and J. Xu. 2001. The causes of land-use and land-cover change: moving beyond the myths. *Global Environmental Change* 11: 261 – 269.

Lane, S.N., J.H. Chandler, and K.S. Richards. 1994. Developments in monitoring and terrain modelling small scale riverbed topography. *Earth Surface Processes and Landforms* 19(4): 349–368.

Lane, S.N., K.S. Richards, and J.H. Chandler. 1996. Discharge and sediment supply controls on erosion and deposition in a dynamic alluvial channel. *Geomorphology* 15(1): 1–15.

Lane, S.N. 1998. The use of digital terrain modelling in the understanding of dynamic river channel systems. *Landform monitoring, modelling, and analysis* 311–342.

Lane, S.N. 2000. The measurement of river channel morphology using digital photogrammetry. *Photogrammetric Record* 16(96): 937 – 1961.

Lewin, J., and M.M.M. Manton. 1975. Welsh floodplain studies: the nature of floodplain geometry. *Journal of Hydrology* 25(1): 37–50.

Lhuillier, M., and L. Quan. 2005. A quasi-dense approach to surface reconstruction from uncalibrated images. *IEEE Trans. Pattern Analysis and Machine Intelligence,* 27: 418 – 433.

Li, J., E. Li, Y. Chen, L. Xu, and Y. Zhang. 2010. Bundled depth-map merging for Multi-View Stereo. *IEEE Conference, Computer Vision and Pattern Recognition* June 2010: 2769 – 2776. San Francisco, CA.

Lowe, D.G. 1999. Object recognition from local scale-invariant keypoints. *International Conference on Computer Vision,* September 1999: 1150 – 1157. Corfu, Greece.

Lowe, D.G. 2001. Local feature view clustering for 3D object recognition. *Proceedings of the IEEE Conference on Computer Vision and Pattern Recognition,* 2001: 7. Kauai, Hawaii.

Lowe, D.G. 2004. Distinctive image features from scale-invariant keypoints. *International Journal of Computer Vision*, 60: 91 – 110.

Luhmann, T., S. Robson, S. Kyle, and J. Boehm. 2013. *Close Range Photogrammetry: 3D Imaging Techniques*. Germany: Walter De Gruyter Inc.

Lucas, B.D. and T. Kanade. 1981. An iterative image registration technique with an application in stereo vision. *International Joint Conference on Artificial Intelligence,* April 1981: 674 – 679. Vancouver, British Columbia.

Matas, J., O. Chum, M. Uban, and T. Pajdla. 2004. Robust wide baseline stereo from maximally stable extremal regions. *Image and Vision Computing* 2210: 761 – 767.

Micheletti, N., J.H. Chandler, and S.N. Lane. 2015 Structure from Motion Photogrammetry. *Geomorphological Techniques* Ch.2: Sec. 2.2

Mikolajczyk, K., T. Tuytelaars, and C. Schmid et al. 2005. A comparison of affine region detectors. *International Journal of Computer Vision* 65(1/2): 43 – 72.

Monroe, A.P., C.L. Aldridge, M.S. O'Donnell, D.J. Mnaier, C.G. Homer, and P.J. Anderson. 2020. Using remote sensing products to predict recovery of vegetation across space and time following energy development. *Ecological Indicators* 110.

Moravec, H. 1983. The Stanford cart and the CMU rover. *Proceedings of the IEEE*, 71(7): 872-884.

Mosbrucker, A.R., J.J. Major, K.R. Spicer, and J. Pitlick. 2017. Camera system considerations for geomorphic applications of SfM photogrammetry. *USGS Staff Published Research*: 1007.

Mulholland, P.J. 2004. Stream ^{15}N Experiment Protocols. In: *Lotic Intersite Nitrogen Experiment II (LINXII)* Ch. 4a: 25 – 30 (https://lter.kbs.msu.edu/research/areas-of-research/lotic-intersite-nitrogen-experiment-linx/) (Last accessed 11 November 2019)

National Aeronautics and Space Administration. 2013. Putting Landsat 8's Bands to Work. https://landsat.gsfc.nasa.gov/landsat-8/landsat-8-bands/ (last accessed 10 November 2019).

Natural Resource Conservation Service. 2010. Natural channel and floodplain restoration, *Applied Fluvial Geomorphology*.

Naiman, R.J., H. Decamps, and M. Pollock. 1993. The role of riparian corridors in maintaining regional biodiversity. *Ecological Applications* 3(2): 209-212.

Naumen, T.W., M.C. Duniway, M.L. Villarreal, and T.B. Poitras. 2017. Disturbance automated reference toolset (DART): Assessing patterns in ecological recovery from energy development on the Colorado Plateau. *Science Total Environment* 476 – 488, 584 – 585.

Nilson, C., R. Jansson, and U. Zinko. 1997. Long-term responses of river-margin vegetation to water-level regulation. *Science* 276: 798-800.

Noble, T. 2018. Photoscan expert workflow. Workshop materials dated October 2018. U.S. Bureau of Land Management.

Oetter, D.R., S.V. Gregory, L.R. Ashkenas, and P.J. Minear. 2004. GIS methodology for characterizing historical conditions of the Willamette River flood plain, Oregon. *Transactions in GIS*, 8: 367-383.

Pickett, S.T.A., and V.T. Parker. 1994. Avoiding the old pitfalls: Opportunities in a new discipline. *Restoration Ecology* 2(2): 75 – 79.

Peterson, E., M. Klein, and R. Stewart. 2015. Whitepaper on Structure from Motion Photogrammetry: Constructing Three Dimensional Models from Photography. U.S. Department of the Interior, Bureau of Reclamation, October, 2015. Weaverville, CA.

Rosgen. D.L. 1994. A classification of natural rivers. *Catena* 22(3): 169 – 199.

Rosnell, T., and E. Honkavaara. 2012. Point cloud generation from aerial image data acquired by quadrocopter type micro unmanned aerial vehicle and a digital still camera. *Sensors* 12: 453 – 480.

Seitz, S.M., and C. Dyer. 1999. Photorealistic scene reconstruction by voxel coloring. *International Journal of Computer Vision* 35(2): 151 – 173.

Smith, M.W., J.L. Carrivick, and D.J. Quincey. 2016. Structure from Motion photogrammetry in physical geography. *Progress in Physical Geography* 40(2): 247 – 275.

Snavely, N., S.N. Seitz, and R. Szeliski. 2008. Modeling the world from internet photo collections. *Internet Journal of Computer Vision* 80: 189-210.

Strahler, A.N. 1952. Dynamic basis of geomorphology. *Bulletin of the Geological Society of America* 63(9): 923–938.

Stumpf, A., J.P. Malet, P. Alleman, M. Pierrot-Deseillingny, and G. Skupinski. 2015. Ground-based multi-view photogrammetry for monitoring of landslide deformation and erosion. *Geomorphology* 231: 130-145.

Szeliski, R. 2011. *Computer Vision: Algorithms and Applications.* London: Springer.

Thompson, EH. 1965. Review of methods independent model aerial triangulation. *The Photogrammetric Record* 5: 72–79.

Thompson, W.H., and P.L. Hansen. 2001. Classification and management of riparian and wetland sites of the Saskatchewan prairie ecozone and parts of adjacent subregions. *Saskatchewan Wetland Conservation Corporation*: 298. Regina, Saskatchewan, Canada.

Triggs, B., P.F. McLauchlan, R.I. Hartley, and A.W. Fitzgibbon. 2000. Bundle adjustment – a modern synthesis. In: Triggs, B., Zisserman, A. & Szeliski R. (eds), *Vision Algorithms '99,* 1883: 298 – 372. Springer-Verlag, Berlin Heidelberg.

Ullman, S. 1979. The interpretation of Structure from Motion. *Proceedings of the Royal Society B.* 203: 405 – 426.

U.S. Department of Agriculture. 2007. Part 654 Stream Restoration Design. In: *National Engineering Handbook*.

U.S. Environmental Protection Agency. 2016 Second Five-Year Review Report for the Milltown Reservoir/Clark Fork River Superfund Site - EPA ID MTD980717565. https://semspub.epa.gov/work/08/1551844.pdf (last accessed 1 November 2019).

Wen, Z., M. Ma, C. Zhang, X. Yi, J. Chen, and S. Wu. 2017. Estimating seasonal aboveground biomass of riparian pioneer plant community: An exploratory analysis by canopy structural data. *Ecological Indicators* 83: 441 – 450.

Westoby, M.J., J. Brasington, N.F. Glasser, M.J. Hambrey, and J.M. Reynolds. 2012. "Structure-from-Motion photogrammetry": A low-cost, effective tool for geoscience applications. *Geomorphology* 179: 300 – 314.

White, P.S., and J.L. Walker. 1997. Approximating nature's variation: Selecting and using reference information in restoration ecology. *Restoration Ecology* 5(4): 338 – 349.

Wolf, P. 1974. *Elements of Photogrammetry (with Air Photo Interpretation and Remote Sensing)*. New York: McGraw-Hill.

Young, E.J. 2013. Section 2.1.3: dGPS. *Geomorphological Techniques (Online Edition)* London: British Society for Geomorphology.